Trisections and Ozsváth-Szabó Four-Manifold Invariants

by

William E. Olsen

(Under the Direction of David T. Gay)

Abstract

Given a smooth, compact four-manifold X, we demonstrate how to use the data of a trisection map $\pi : X^4 \to \mathbb{R}^2$ to compute the induced cobordism maps on Heegaard Floer homology. A result of Gay and Kirby shows that such a map π induces an open book decomposition on the boundary of X, and we show how to recover the Ozsváth-Szabó contact invariant in this setting, along with its image under the cobordism maps.

Index words: Trisections of four-manifolds, Heegaard Floer homology

Trisections and Ozsváth-Szabó Four-Manifold Invariants

by

William E. Olsen

B.S., University of North Florida, 2012

M.S., University of North Florida, 2014

A Dissertation Submitted to the Graduate Faculty of the

University of Georgia in Partial Fulfillment of the Requirements for the Degree.

Doctor of Philosophy

Athens, Georgia

2020

Trisections and Ozsváth-Szabó Four-Manifold Invariants

by

William E. Olsen

Major Professor: David T. Gay

Committee: Michael Usher
Gordana Matić
Peter Lambert-Cole

Electronic Version Approved:

Ron Walcott
Interim Dean of the Graduate School
The University of Georgia
August 2020

Dedication

To my wife, Shelby, and to my mother, Eileen.

ACKNOWLEDGEMENTS

I would like to thank my advisor, David Gay, for his continued support and encouragement. Without his extended guidance and mentorship, this thesis would not have been possible. The math department at UGA has been a fun and supportive place to do mathematics, and I would like to thank the community here for making my experience as a graduate student so memorable. Special thanks go to thank Michael Usher, Neil Lyall, Ted Shifrin, and Laura Ackerley for their support and mentorship. I am also grateful to the Max Planck Institute for Mathematics in Bonn, Germany, for providing a stimulating and exciting workplace environment. Finally, I would never have reached this point without the strong and continual support of my family: my parents, Craig and Eileen, my sister Sara, my brother Kevin, and my wife Shelby. Thank you.

Contents

List of Figures

Chapter 1

Introduction

The study of generic smooth maps from four-manifolds to surfaces has greatly deepened our understanding of the topology of smooth four-manifolds. A new tool in this field has recently been introduced under the name of *trisected Morse* 2*-functions* (or *trisections* for short) by Gay and Kirby [GK16]. The trisection theory has been shown to have rich connections and applications to other aspects of four-manifold topology, including surface knots [MZ17; MZ18], surgery operations such as the gluck twist and its variants [GM18; KM20], and to symplectic geometry [LMS20; Lam19; LM18].

Equipped with a new tool with which to study four-manifolds, it is natural to demonstrate connections to more familiar techniques and approaches. Given X, a smooth, oriented, connected, compact 4-manifold with $b_2^+(X) \geq 2$, our aim in this thesis is to demonstrate a technique for computing the Ozsváth-Szabó four-manifold invariants which arise in Heegaard Floer homology [OS04b; OS06]. To do so, we follow the usual Mayer-Vietoris strategy which is common in Floer theories; namely, we decompose X into two pieces $X = X_1 \cup_Y X_2$ where each X_i has $b_2^+(X_i) > 0$ and $Y = \partial X_1 = -\partial X_2$ is a separating three-manifold for which $\delta : H^1(Y) \to H^2(X)$ is injective[1]. Viewing the punctured X_1 as a cobordism from S^3 to

[1]Such a three-manifold Y is referred to as an *admissable cut* [OS06, Definition 8.10]. Here, $\delta : H^1(Y) \to H^2(X)$ is the connecting homomorphism in the Mayer-Vietoris cohomology sequence associated to the decomposition $X = X_1 \cup_Y X_2$.

Y, and the punctured X_2 as a cobordism from Y to S^3, we demonstrate how, starting with the data of a trisection map on each of the X_i, to compute the induced cobordism maps of Ozsváth and Szabó (see Theorem 4.9 for a precise statement).

Theorem 1.1. *Fix a smooth, connected, oriented, compact four-manifold X with connected boundary $\partial X = Y$, and let $\pi : X \to \mathbb{R}^2$ be a (relative) trisection map. Using π as input data, one can recover the induced cobordism maps in Heegaard Floer homology*

$$F^{\circ}_{X,\mathfrak{s}} : HF^{\circ}(S^3) \to HF^{\circ}(Y, \mathfrak{s}|_Y), \tag{1.1}$$

where $\circ \in \{+, -, \infty, \wedge\}$ are the variants defined in [OS04b].

Once we've established Theorem 1.1 in Section 4.3 the mixed invariants follow quickly in the usual way [OS06], see Section 4.1 for more details.

A trisection map $\pi : X \to \mathbb{R}^2$ on a four-manifold with boundary X contains more information than simply a handle-decomposition. Indeed a result of [GK16] shows that π induces an open book decomposition of its boundary three-manifold Y, and a theorem of Giroux states that there is a one-to-one correspondence between contact structures up to isotopy and open book decompositions up to positive stabilization [Gir02]. By [HKM09, Theorem 3], one can associate to this open book decomposition a class $c^+(\xi) \in HF^+(-Y, \mathfrak{s}_\xi)$, known as the *contact class* originally defined by Ozsváth and Szabó [OS05] where it is proven that $c^+(\xi)$ is an invariant of the contact isotopy class of ξ. In the process of proving Theorem 1.1, we also demonstrate:

Theorem 1.2. *Let X be as above. Using the data of a (relative) trisection map $\pi : X \to \mathbb{R}^2$, one can compute the image of the contact class $c^+(\xi)$ under the cobordism map*

$$F^{+}_{\overline{X},\overline{\mathfrak{s}}} : HF^{+}(-Y, \overline{\mathfrak{s}}|_Y) \to HF^{+}(S^3), \tag{1.2}$$

where $\overline{X}$ is X 'turned around', and $\overline{\mathfrak{s}}$ is the conjugate Spin^c-structure.

See Theorem 4.11 for a precise statement. Theorem 1.2 has the potential for many new applications. In [AK11; Won16], the authors exhibit the exotic behavior of 4-manifolds under cork and G-cork twists by proving these diffeomorphisms act non-trivially on the contact invariant of the boundary 3-manifold. Additionally, Juhász and Zemke [JZ18a] use a similar idea to compute the effect of concordance surgery [Akb02], a generalization of Fintushel-Stern knot surgery [FS98], in Heegaard Floer homology. The simplifications utilized in the papers above, which amount to factoring the Heegaard Floer cobordism maps through the contact element of 3-manifolds with small Heegaard Floer rank, should also expand the applicability of Theorems 1.1 and 1.2. In particular, combining these simplifications with the symmetry inherent in the trisection pictures gives hope to being able to perform new and interesting computations.

Organization

The remainder of this thesis is organized as follows. In Sections 2 and 3, we review the essential theorems and results arising in both the trisection theory and Heegaard Floer homology. With these preliminaries in place, we demonstrate in Section 4 how to effectively use the data of a relative trisection map to compute the Ozsváth-Szabó cobordism maps.

Chapter 2

Trisections of four-manifolds

The literature is rich with helpful and insightful constructions of the trisection theory. For this reason, we only briefly review its foundational material and point the interested reader elsewhere for a less terse introduction. For a general overview of trisections and direct comparisons with the more familiar description of four-manifolds via handle decompositions and Kirby calculus, we recommend the original [GK16] and the more recent survey [Gay19]. For interesting examples of trisections and their diagrams, including descriptions for various surgery operations such as the Gluck twist and its variants, we recommend [KM20; LM18; GM18; AM19] and [Koe17]. For a broader perspective on stable maps from four-manifolds to surfaces, including details about how to simplify the topology of such maps, we suggest [GK15; GK12; BS17] and the references therein.

2.1 Trisections, connections, and parallel transport

Fix X to be a smooth, oriented, connected, closed four-manifold.

Definition 2.1. A $(g; \mathbf{k})$-*trisection* of X is a decomposition into three pieces $X = Z_1 \cup Z_2 \cup Z_3$ such that the following conditions are satisfied

(T1) Each Z_i is diffeomorphic to $\natural^{k_i} S^1 \times \mathbb{D}^3$ where $\mathbf{k} = (k_1, k_2, k_3)$ is a tuple of non-negative integers.

(T2) Each double intersection $U_i := Z_i \cap Z_{i-1}$ is a three-dimensional handlebody of genus g; and,

(T3) the triple intersection $\Sigma := Z_1 \cap Z_2 \cap Z_3$ is a closed, oriented surface of genus g.

We refer to the union $\mathcal{S} = U_1 \cup U_2 \cup U_3$ as the *spine* of the trisection, and we call the distinguished surface Σ the *central surface*. According to classic results of Laudenbach and Poenaru [LP72], the data of a trisection can be completely recovered from its spine.

The theory of trisections arose from the study of generic smooth maps from four-manifolds to surfaces [GK12; GK15; GK16]. We now explain this perspective and along the way explain how the familiar notions of connection, parallel transport, and vanishing cycles can be imported into this setting. To be clear, none of what's presented in this section is original, our main sources being the excellent work [Hay14; BH12; BH16; Beh14].

A (g, k)-*trisection map* $\pi : X \to \mathbb{R}^2$ is a stable map whose critical image is shown in Figure 2.1 below. The stability of π implies that its critical locus and critical image admit standard local coordinate descriptions of the following three types:

1. *Indefinite fold model*: in local coordinates, π is equivalent to:

$$(t, x, y, z) \mapsto (t, x^2 + y^2 - z^2) \tag{2.1}$$

2. *Indefinite cusp model*: in local coordinates, π is equivalent to

$$(t, x, y, z) \mapsto (t, x^3 + 3tx + y^2 - z^2) \tag{2.2}$$

3. *Definite fold model*: in local coordinates, π is equivalent to:

$$(t, x, y, z) \mapsto (t, x^2 + y^2 + z^2) \tag{2.3}$$

It is advantageous to view a (g, k)-trisection map $\pi : X \to \mathbb{R}^2$ as being a type of singular fibration, so that the preimage of a regular value is a closed, connected surface. We describe how the topology of this fiber changes as one traverses across this critical image after we've incorporated a suitable notion of parallel transport into this picture.

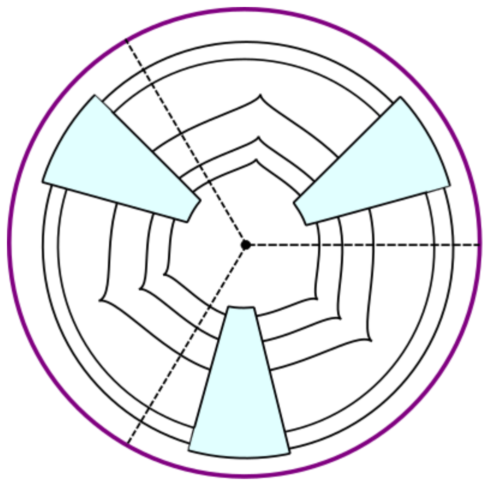

Figure 2.1: The critical image of a trisection map. Curves drawn in black denote indefinite fold circles and indefinite cusps. The solid purple circle denotes a single definite fold.

From a (g, k)–trisection map $\pi : X \to \mathbb{D}^2$ one can recover the decomposition described in Definition 2.1. Clearly, the three dotted line segments in Figure 2.1 decompose the image of π into three sectors D_1, D_2, and D_3. Define $Z_i := \pi^{-1}(D_i)$, and note that the local models described in equations (2.1)–(2.3) imply that

$$X = Z_1 \cup Z_2 \cup Z_3$$

is naturally a (g, k)–trisection of X, where $\pi^{-1}(0, 0) = \Sigma$ is the central surface (see [GK16, Section 3] for more details).

In Section 4, we will need a tool for comparing different regular fibers of a given (g,k)-trisection map. For this, we review some familiar notions.

Definition 2.2. Let $\pi : X \to \mathbb{R}^2$ be a (g,k)-trisection map. A *π-compatible connection* (or *π-connection* for short) is a subset $\mathcal{H} \subset TX$ defined as the pointwise orthogonal complement of $\ker(d\pi)$ with respect to some Riemannian metric on X.

If we restrict a given $\pi : X \to \mathbb{R}^2$ to a region which misses the critical locus, then we recover the usual definition of a connection for a fiber bundle. To specify what happens as we traverse the critical image, we establish some preliminary terminology.

Definition 2.3. Let $\pi : X \to \mathbb{R}^2$ be a (g,k)-trisection map.

- A *reference arc* is an embedded arc $\eta : [0,1] \to \mathbb{R}^2$ such that both $\eta(0)$ and $\eta(1)$ are regular values of π.
- Given a π-compatible connection $\mathcal{H}$, an *$\mathcal{H}$-lift* of the reference arc $\eta : [0,1] \to \mathbb{R}^2$ is a map $\widetilde{\eta} : \mathcal{O} \to X$ which satisfies
  - $\big(\pi \circ \widetilde{\eta}\big)(t) = \eta(t)$ for all $t \in \mathcal{O}$, where $\mathcal{O} \subset [0,1]$ is a relatively open subinterval, and
  - the tangent vectors of $\widetilde{\eta}$ are contained in $\mathcal{H}$.

Next, we discuss parallel transport, for which we need the following crucial proposition. See [Hay14] for a proof.

Proposition 2.4. *Let $\pi : X \to \mathbb{R}^2$ be a (g,k)-trisection map equipped with a π-connection $\mathcal{H}$, and let $\eta : [0,1] \to \mathbb{R}^2$ be a reference arc for π and $p \in \Sigma_t$ a regular point from some fixed $t \in [0,1]$.*

1. *There exists a unique $\mathcal{H}$-lift of η, denoted by*

$$\widetilde{\eta}^{\mathcal{H}}_{t,p} : \mathcal{O}_{t,p} \to X, \quad \mathcal{O}_{t,p} \subset [0,1],$$

where $\mathcal{O}_{t,p}$ is a relatively open interval containing t such that $\widetilde{\eta}^{\mathcal{H}}_{t,p}(t) = p$ and all other $\mathcal{H}$-lifts of γ with this property are restrictions of $\widetilde{\eta}^{\mathcal{H}}_{t,p}$.

2. *If $\mathcal{H}$ depends smoothly on some auxiliary parameters, then so does $\widetilde{\eta}^{\mathcal{H}}_{t,p}$.*

3. *If each fiber of π along η contains at most finitely many critical points of π, then $\widetilde{\eta}^{\mathcal{H}}_{t,p}$ limits to a critical point on each open end of $\mathcal{O}_{t,p}$.*

A reference arc $\eta : [0,1] \to \mathbb{R}^2$ for a given (g,k)-trisection map $\pi : X \to \mathbb{D}^2$ is called a *fold reference arc* if it transversely intersects the critical image of π in a single fold value. Given a fold reference arc $\eta : [0,1] \to \mathbb{D}^2$ and a critical point $q \in \pi^{-1}(\eta) \cap \mathsf{Crit}(\pi)$, we say that $\widetilde{\eta}^{\mathcal{H}}_{t,p}$ *runs into* q (or *emerges from* q) if its left (or right) limit is q. We can now define what we call the *vanishing sets* of the triple $(\eta, \mathcal{H}; q)$ as

$$V_0(\eta, \mathcal{H}; q) = \{p \in \Sigma_0 | \widetilde{\eta}^{\mathcal{H}}_{0,p} \text{ runs into } q\} \subset \Sigma_0$$
$$V_1(\eta, \mathcal{H}; q) = \{p \in \Sigma_1 | \widetilde{\eta}^{\mathcal{H}}_{1,p} \text{ emerges from } q\} \subset \Sigma_1. \tag{2.4}$$

We often write $V_0 \subset \Sigma_0$ and $V_1 \subset \Sigma_1$ for the unions $V_i(\eta, \mathcal{H}; q)$ over all $q \in \pi^{-1}(\eta) \cap \mathsf{Crit}(\pi)$. We define *parallel transport* along η with respect to a fixed π-connection $\mathcal{H}$ by

$$\Pi^{\mathcal{H}}_{\eta} : \Sigma_0 \setminus V_0 \to \Sigma_1 \setminus V_1, \qquad p \mapsto \widetilde{\eta}^{\mathcal{H}}_{0,p}(1) \tag{2.5}$$

By the indefinite fold model (2.1), it follows that $\pi^{-1}(\eta)$ is a smooth three-manifold and that $\eta^{-1} \circ \pi : \pi^{-1}(\eta) \to [0,1]$ is a Morse function with a single critical point of index 1 or 2 depending on the direction in which η crosses the fold arc. If the index is 2, then the vanishing sets with respect to any connection $\mathcal{H}$ consist of a simple closed curve $c \subset \Sigma_0$ and a pair of points $\{p, q\} \subset \Sigma_1$. Due to its similarity with the theory of Lefschetz fibrations, c is usually referred to as a *vanishing cycle.*

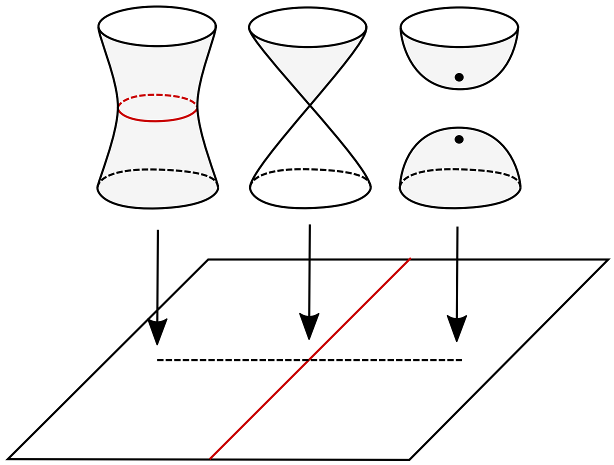

Figure 2.2: A vanishing cycle for an indefinite fold.

Observe that parallel transport along η with respect to a given π-connection $\mathcal{H}$ yields a preferred diffeomorphism

$$\Pi_\eta^{\mathcal{H}} : \Sigma_0 \setminus c \to \Sigma_1 \setminus \{p, q\}.$$

The above diffeomorphism is an identification of Σ_1 with the surface obtained from Σ after surgery along c as follows. The surgery of Σ along c can be identified with the endpoint compactification of $\Sigma_0 \setminus c$ while the endpoint compactification of $\Sigma_1 \setminus \{p, q\}$ is canonically identified with Σ_1. Moreover, $\Pi_\gamma^{\mathcal{H}}$ extends to a diffeomorphism of the endpoint compactifications. As a consequence, we see that the vanishing cycle $c \subset \Sigma$ must be non-separating and Σ_1 has genus one lower than Σ_0.

Note that the specific vanishing sets and parallel transport diffeomorphisms depend on both η and $\mathcal{H}$. It is therefore important to understand this dependence.

Lemma 2.5. *Let $\pi : X \to \mathbb{R}^2$ be a (g, k)-trisection map. For $s \in [0, 1]$ we consider smooth families of connections $\mathcal{H}_s$ and fold reference arcs $\eta_s : [0, 1] \to \mathbb{R}^2$ with common endpoints. Then the vanishing sets $c_s \subset \Sigma_0$ and $\{p_s, q_s\} \subset \Sigma_1$ evolve by ambient isotopies. Moreover, all ambient isotopies of $c_0 \subset \Sigma_0$ and $\{p_0, q_0\} \subset \Sigma_1$ can be realized by changing each $\mathcal{H}_s$ in an arbitrarily small neighborhood of $\pi^{-1}(\eta_s)$.*

Next, we extend our discussion to compact four-manifolds with non-empty boundary. To this end, let X be a smooth, connected, compact, oriented 4-manifold with connected boundary $\partial X = Y$. A *relative* $(g, k; p, b)$*-trisection map* $f : X^4 \to \mathbb{D}^2$ is a stable map with critical image consisting of round indefinite folds and cusps, as in the closed case Figure 2.1, but in addition we impose certain regularity conditions near the boundary of X.

1. The boundary of X decomposes as $\partial X = \partial^v X \cup \partial^h X$, where $\partial^v X$ and $\partial^h X$ are codimension zero submanifolds of ∂X and are glued along their respective boundaries.

2. X has corners exactly along $\partial^h X \cap \partial^v X$.

3. $\pi^{-1}(\partial \mathbb{D}^2) = \partial^v X$.

4. $\pi|_{\partial^v X} : \partial^h X \to \partial \mathbb{D}^2$ and $\pi|_{\partial^h X} : \partial^h X \to \mathbb{D}^2$ are both submersions.

5. *Horizontality of* $\partial^h X$*.* If x lies in $\partial^h X$, then the horizontal part of the tangent space lies in $T_x \partial^h X$.

In [GK16], Gay and Kirby show that such a stable map on a four-manifold with connected boundary induces an open book decomposition.

Theorem 2.6. *A relative* $(g, k; p, b)$*-trisection map* $\pi : X \to \mathbb{D}^2$ *induces an open book decomposition on the boundary three-manifold.*

The above discussion of connections and parallel transport can be quickly adapted to the case when X has nonempty boundary. For example, if $\eta : [0, 1] \to \mathbb{D}^2$ is an embedded arc in $\mathbb{D}^2$ which is transverse to the critical image of π, then $\eta^{-1} \circ \pi : \pi^{-1}(\eta) \to [0, 1]$ is a Morse function. As π is a submersion on $\partial^v X$, the fibers are compact surfaces with boundary and this Morse function is a submersion on the closure of the boundary of $\pi^{-1}(\eta)$. So we can choose a gradient-like vector field that is tangent to the boundary. This means that an integral curve never hits the boundary (except along $\pi^{-1}(\partial \eta)$) as long as we start from an interior point.

2.2 Diagrammatic representations of manifolds

The theory of trisections of four-manifolds is analogous to that of Heegaard splittings of three-manifolds, and since Heegaard diagrams are the diagrammatic input for Heegaard Floer homology, it makes sense to introduce them along with trisection diagrams side-by-side. This section closely follows [GM18, Section 2.2].

Definition 2.7. A *cut system* on a closed, connected, oriented, genus g surface Σ is a collection of g disjoint simple closed curves $\boldsymbol{\delta} = \{\delta_1, \ldots, \delta_g\} \subset \Sigma$ which are linearly independent in $H_1(\Sigma_g; \mathbb{Z})$. Two cut systems are *slide-equivalent*[1] if they are related by a sequence of handleslides. Two tuples $(\Sigma, \boldsymbol{\delta} = \{\delta_1, \ldots, \delta_g\})$ and $(\Sigma', \boldsymbol{\delta}' = \{\delta'_1, \ldots, \delta'_g\})$, where $\boldsymbol{\delta}$ and $\boldsymbol{\delta}'$ are cut systems, are *slide-diffeomorphic* if there is a diffeomorphism $\phi : \Sigma \to \Sigma'$ such that $\phi(\boldsymbol{\delta})$ is slide-equivalent to $\boldsymbol{\delta}'$.

A cut system $\boldsymbol{\delta}$ on Σ determines (up to diffeomorphism rel. boundary) a handlebody $H_{\boldsymbol{\delta}}$ with $\partial H_{\boldsymbol{\delta}} = \Sigma$, and every handlebody H with boundary the given surface Σ arises in this way. Finally, $H_{\boldsymbol{\delta}}$ and $H_{\boldsymbol{\delta}'}$ are diffeomorphic rel. boundary if and only if $\boldsymbol{\delta}$ and $\boldsymbol{\delta}'$ are slide-equivalent.

Definition 2.8. A *Heegaard diagram* is a triple $(\Sigma, \boldsymbol{\alpha}, \boldsymbol{\beta})$ where Σ is a surface and each of $\boldsymbol{\alpha} = \{\alpha_1, \ldots, \alpha_g\}$ and $\boldsymbol{\beta} = \{\beta_1, \ldots, \beta_g\}$ are cut systems on Σ. A *Heegaard triple* is a 4-tuple $(\Sigma, \boldsymbol{\alpha}, \boldsymbol{\beta}, \boldsymbol{\gamma})$ where Σ is a surface and each of $\boldsymbol{\alpha}, \boldsymbol{\beta}$, and $\boldsymbol{\gamma}$ are cut systems on Σ. A (g, k)-*trisection diagram* is a Heegaard triple $(\Sigma, \boldsymbol{\alpha}, \boldsymbol{\beta}, \boldsymbol{\gamma})$ where each tuple $(\Sigma, \boldsymbol{\alpha}, \boldsymbol{\beta})$, $(\Sigma, \boldsymbol{\beta}, \boldsymbol{\gamma})$, and $(\Sigma, \boldsymbol{\gamma}, \boldsymbol{\alpha})$ are each slide-diffeomorphic to the standard genus g Heegaard splitting of $\#^k S^1 \times S^2$.

It is well-known that Heegaard diagrams and Heegaard triples determine smooth 3- and 4-manifolds, up to diffeomorphism. We review the construction for Heegaard triples, and make comments about the special case of a trisection diagram.

[1] In the Heegaard Floer literature, it is common to use the term *strongly equivalent*.

Let $H = (\Sigma, \boldsymbol{\alpha}, \boldsymbol{\beta}, \boldsymbol{\gamma})$ be a Heegaard triple. In [OS04b, Section 8], Ozsváth and Szabó associate to H a four-manifold $X_{\boldsymbol{\alpha},\boldsymbol{\beta},\boldsymbol{\gamma}}$ via

$$X_{\boldsymbol{\alpha},\boldsymbol{\beta},\boldsymbol{\gamma}} := \Big((\Sigma \times \Delta) \cup (U_{\boldsymbol{\alpha}} \times e_{\boldsymbol{\alpha}}) \cup (U_{\boldsymbol{\beta}} \times e_{\boldsymbol{\beta}}) \cup (U_{\boldsymbol{\gamma}} \times e_{\boldsymbol{\gamma}})\Big) / \sim \tag{2.1}$$

where Δ is a triangle with edges labeled $e_{\boldsymbol{\alpha}}, e_{\boldsymbol{\beta}}$, and $e_{\boldsymbol{\gamma}}$ clockwise, and $\sim$ is the relation determined by gluing $U_{\boldsymbol{\tau}} \times e_{\boldsymbol{\tau}}$ to $\Sigma \times \Delta$ along $\Sigma \times e_{\boldsymbol{\tau}}$ for each $\boldsymbol{\tau} \in \{\boldsymbol{\alpha}, \boldsymbol{\beta}, \boldsymbol{\gamma}\}$ using the natural identification.

We note that if $H = (\Sigma, \boldsymbol{\alpha}, \boldsymbol{\beta}, \boldsymbol{\gamma})$ is a general Heegaard triple, with no conditions on the pairwise cut systems, then the four-manifold $X_{\boldsymbol{\alpha},\boldsymbol{\beta},\boldsymbol{\gamma}}$ constructed in equation (2.1) has three boundary components

$$\partial X_{\boldsymbol{\alpha},\boldsymbol{\beta},\boldsymbol{\gamma}} = -Y_{\boldsymbol{\alpha},\boldsymbol{\beta}} \sqcup -Y_{\boldsymbol{\beta},\boldsymbol{\gamma}} \sqcup Y_{\boldsymbol{\alpha},\boldsymbol{\gamma}} \tag{2.2}$$

given by the three Heegaard splittings $(\Sigma, \boldsymbol{\alpha}, \boldsymbol{\beta})$, $(\Sigma, \boldsymbol{\beta}, \boldsymbol{\gamma})$, and $(\Sigma, \boldsymbol{\gamma}, \boldsymbol{\alpha})$.

However, if $H = (\Sigma, \boldsymbol{\alpha}, \boldsymbol{\beta}, \boldsymbol{\gamma})$ is required to be a trisection diagram, so that we have

$$(\Sigma, \boldsymbol{\alpha}, \boldsymbol{\beta}) \cong (\Sigma, \boldsymbol{\beta}, \boldsymbol{\gamma}) \cong (\Sigma, \boldsymbol{\gamma}, \boldsymbol{\alpha}) \cong \#^k S^1 \times S^2,$$

then it follows (again from Laudenbach-Poenaru [LP72]) that we can fill in these three boundary components and obtain a closed four-manifold.

Now, we move on to reviewing the diagrammatics of compact four-manifolds with connected boundary.

Definition 2.9. A *genus p cut system* on a compact, connected, orientable genus g surface Σ with b boundary components is a collection of $g - p$ disjoint simple closed curves on Σ which collectively cut Σ into a connected genus p surface. The notions of *slide-equivalence* carry over.

In this more general setting, a genus p cut system on a genus g surface Σ with b boundary components determines (up to diffeomorphism rel. boundary) a compression body $C_{\boldsymbol{\delta}}$ with $\partial C_{\boldsymbol{\delta}} = \Sigma \cup (I \times \partial\Sigma) \cup \Sigma_{\boldsymbol{\delta}}$, where $\Sigma_{\boldsymbol{\delta}}$ is the result of surgering Σ along $\boldsymbol{\delta}$.

Definition 2.10. A $(g, \mathbf{k}; p, b)$-*relative-trisection diagram* is a 4-tuple $(\Sigma, \boldsymbol{\alpha}, \boldsymbol{\beta}, \boldsymbol{\gamma})$ where Σ is a genus g compact, connected surface with b boundary components, $\boldsymbol{\alpha}$, $\boldsymbol{\beta}$, and $\boldsymbol{\gamma}$ are genus p cut systems on Σ, and each of $(\Sigma, \boldsymbol{\alpha}, \boldsymbol{\beta})$, $(\Sigma, \boldsymbol{\beta}, \boldsymbol{\gamma})$, and $(\Sigma, \boldsymbol{\gamma}, \boldsymbol{\alpha})$ is slide-diffeomorphic to the trivial $(g, k_i; p, b)$-diagram shown below.

Recall from Section 2.1 that a trisection on a four-manifold induces an open book decomposition of its boundary. By decorating the central surface Σ with additional arcs, we can access this information diagrammatically.

Definition 2.11. Given a genus p cut system $\boldsymbol{\tau}$ on Σ, an *arc system relative to* $\boldsymbol{\tau}$ is a collection $\mathfrak{t}$ of $2p + b - 1$ properly embedded arcs in Σ, disjoint from $\boldsymbol{\tau}$, such that cutting along $\mathfrak{t}$ and surgering along $\boldsymbol{\tau}$ turns Σ into a disk. If $\mathfrak{t}$ and $\mathfrak{t}'$ are arc systems relative to cut systems $\boldsymbol{\tau}$ and $\boldsymbol{\tau}'$, respectively, we say that $(\boldsymbol{\tau}, \mathfrak{t})$ is *slide-equivalent* to $(\boldsymbol{\tau}', \mathfrak{t}')$ if the one can be transformed to the other by ordinary handleslides on the cut systems and by sliding arcs from the arc system over curves from the cut system.

Remark 1. Note that we *do not allow* the sliding of arcs over arcs, nor isotopies that move points on $\partial\Sigma$.

Definition 2.12. An *arced relative trisection diagram* is a tuple $(\Sigma, \boldsymbol{\alpha}, \boldsymbol{\beta}, \boldsymbol{\gamma}; \mathfrak{a}, \mathfrak{b}, \mathfrak{c})$ such that $(\Sigma, \boldsymbol{\alpha}, \boldsymbol{\beta}, \boldsymbol{\gamma})$ is a relative trisection diagram, $\mathfrak{a}$ (resp. $\mathfrak{b}$, resp. $\mathfrak{c}$) is an arc system relative to $\boldsymbol{\alpha}$ (resp. $\boldsymbol{\beta}$, resp. $\boldsymbol{\gamma}$) and such that we have the following pairwise standardness conditions

1. $(\Sigma, \boldsymbol{\alpha}, \boldsymbol{\beta}, \mathfrak{a}, \mathfrak{b})$ is slide-equivalent to some $(\Sigma, \boldsymbol{\alpha}', \boldsymbol{\beta}', \mathfrak{a}', \mathfrak{b}')$ such that $(\Sigma, \boldsymbol{\alpha}', \boldsymbol{\beta}')$ is diffeomorphic to the trivial $(g, k_i; p, b)$-diagram and $\mathfrak{a}' = \mathfrak{b}'$.

2. $(\Sigma, \boldsymbol{\beta}, \boldsymbol{\gamma}, \mathfrak{b}, \mathfrak{c})$ is slide-equivalent to some $(\Sigma, \boldsymbol{\beta}', \boldsymbol{\gamma}', \mathfrak{b}', \mathfrak{c}')$ such that $(\Sigma, \boldsymbol{\beta}', \boldsymbol{\gamma}')$ is diffeomorphic to the trivial $(g, k_i; p, b)$-diagram and $\mathfrak{b}' = \mathfrak{c}'$.

Observe that $\partial\mathfrak{a} = \partial\mathfrak{b} = \partial\mathfrak{c}$.

Definition 2.13. A *completed arced relative trisection diagram* is a tuple $(\Sigma, \boldsymbol{\alpha}, \boldsymbol{\beta}, \boldsymbol{\gamma}; \mathfrak{a}, \mathfrak{b}, \mathfrak{c}, \mathfrak{a}^*)$ such that $(\Sigma, \boldsymbol{\alpha}, \boldsymbol{\beta}, \boldsymbol{\gamma}; \mathfrak{a}, \mathfrak{b}, \mathfrak{c})$ is an arced diagram and such that $(\Sigma, \boldsymbol{\gamma}, \boldsymbol{\alpha}, \mathfrak{c}, \mathfrak{a}^*)$ is slide-equivalent to some $(\Sigma, \boldsymbol{\gamma}', \boldsymbol{\alpha}'', \mathfrak{c}', \mathfrak{a}')$ such that $(\Sigma, \boldsymbol{\gamma}', \boldsymbol{\alpha}')$ is diffeomorphic to the trivial $(g, k; p, b)$-diagram.

Using the above data, the authors of [CGP18] show that every relative trisection diagram determines uniquely, up to diffeomorphism, the following data:

- a relatively trisected 4-manifold X with non-empty connected boundary, and
- the open book decomposition on ∂X induced by the trisection. Moreover, the page and the monodromy of the open book on ∂X is determined completely by the relative trisection diagram by an explicit algorithm.

Theorem 2.14 ([CGP18])**.** *For any relative trisection diagram $(\Sigma, \boldsymbol{\alpha}, \boldsymbol{\beta}, \boldsymbol{\gamma})$ and any arc system $\mathfrak{a}$ relative to $\boldsymbol{\alpha}$ on Σ, there exist cut systems $\mathfrak{b}$, $\mathfrak{c}$, and $\mathfrak{a}^*$ such that $\mathfrak{D}^* = (\Sigma, \boldsymbol{\alpha}, \boldsymbol{\beta}, \boldsymbol{\gamma}; \mathfrak{a}, \mathfrak{b}, \mathfrak{c}, \mathfrak{a}^*)$ is a completed arced diagram. Furthermore, the open book decomposition is uniquely determined (up to isotopy) by the original relative trisection diagram $\mathfrak{D}$.*

Chapter 3

Background on Heegaard Floer homology

This sections provides a brief review of the aspects of Heegaard Floer homology that will be most important to us. We assume the reader is familiar with the Heegaard Floer canon [OS04b; OS06; Lip06]. However, we start by reviewing a few concepts in order to fix notation, and to emphasize important differences between trisections, especially relative trisections, and the more common 'Heegaard triples'.

3.1 Heegaard Floer chain complexes

Fix a closed, connected, oriented three-manifold Y, and denote by $Spin^c(Y)$ the space of $Spin^c$ structures on Y. Consider a fixed $\mathfrak{s} \in Spin^c(Y)$. In [OS04b], Ozsváth and Szabó use a pointed Heegaard diagram $H = (\Sigma, \boldsymbol{\alpha}, \boldsymbol{\beta}, w)$ depicting Y to construct Lagrangian Floer cohomology groups associated to the two tori

$$\mathbb{T}_{\boldsymbol{\alpha}} = \alpha_1 \times \cdots \times \alpha_g \quad \mathbb{T}_{\boldsymbol{\beta}} = \beta_1 \times \cdots \times \beta_g$$

inside the symmetric product $\mathsf{Sym}^{\mathrm{g}}(\Sigma_{\mathrm{g}})$. There is a natural map $s_w : \mathbb{T}_{\boldsymbol{\alpha}} \cap \mathbb{T}_{\boldsymbol{\beta}} \to Spin^c(Y)$, and we will focus on those intersection points $\mathbf{x}$ which satisfy $s_w(\mathbf{x}) = \mathfrak{s}$. The definition of the Floer groups requires H to satisfy an admissability condition which depends on $\mathfrak{s}$. We also need to choose a suitable (generic) family J of almost complex structures on $\mathsf{Sym}^{\mathrm{g}}(\Sigma_{\mathrm{g}})$. We will write $\mathcal{H}$ for the data (H, J), which we call a *Heegaard pair*.

Given such a pair $\mathcal{H}$, the Heegaard Floer chain complex $CF^\infty(\mathcal{H}, \mathfrak{s})$ is freely generated over $\mathbb{F}_2$ by pairs $[\mathbf{x}, i]$ with $\mathbf{x} \in \mathbb{T}_{\boldsymbol{\alpha}} \cap \mathbb{T}_{\boldsymbol{\beta}}$ and $i \in \mathbb{Z}$, such that $s_w(\mathbf{x}) = \mathfrak{s}$. The differential is given by

$$\partial[\mathbf{x}, i] = \sum_{\substack{y \in \mathbb{T}_{\boldsymbol{\alpha}} \cap \mathbb{T}_{\boldsymbol{\beta}} \\ s_z(\mathbf{y}) = \mathfrak{s}}} \sum_{\substack{\phi \in \pi_2(\mathbf{x}, \mathbf{y}) \\ \mu(\phi) = 1}} \# \mathcal{M}(\phi) \cdot [\mathbf{y}, i - n_z(\phi)]. \tag{3.1}$$

Here, $\pi_2(\mathbf{x}, \mathbf{y})$ is the space of homotopy classes of Whitney disks connecting $\mathbf{x}$ to $\mathbf{y}$, $\mu(\phi)$ is the Maslov index, $\mathcal{M}(\phi)$ is the moduli space of J-holomorphic disks in the class ϕ (modulo the action of $\mathbb{R}$), and $n_z(\phi)$ is the algebraic intersection number of ϕ with the divisor $\{z\} \times \mathsf{Sym}^{g-1}(\Sigma)$ There is an action of $\mathbb{F}_2[U, U^{-1}]$ on CF^∞, where U acts by $U \cdot [\mathbf{x}, i] = [\mathbf{x}, i - 1]$ and decreases relative grading by 2. The other complexes CF^+, CF^-, and $\widehat{CF}$ are obtained from CF^∞ by considering only pairs $[x, i]$ with $i \geq 0, i < 0$, and $i = 0$. All three complexes have an induced $\mathbb{F}_2[U]$-action, which is trivial in the case of $\widehat{CF}$.

We will write $CF^\circ(\mathcal{H}, \mathfrak{s})$ for any of the four flavors of the Heegaard Floer chain complex, and $HF^\circ(\mathcal{H}, \mathfrak{s})$ for the homology groups.

By construction, there is a short exact sequence of $\mathbb{F}_2[U]$-modules

$$0 \to CF^-(\mathcal{H}, \mathfrak{s}) \xrightarrow{\iota} CF^\infty(\mathcal{H}, \mathfrak{s}) \xrightarrow{\pi} CF^+(\mathcal{H}, \mathfrak{s}) \to 0 \tag{3.2}$$

which yields a long exact sequence on homology. We let

$$\delta : HF^+(Y, \mathfrak{s}) \to HF^-(Y, \mathfrak{s}) \tag{3.3}$$

denote the connecting homomorphism. Finally, we define the *reduced Heegaard Floer homology groups* $HF^{\pm}_{\mathsf{red}}(Y,\mathfrak{s})$ to be

$$HF^{-}_{\mathsf{red}}(Y,\mathfrak{s}) := \ker\left(\iota_* : HF^-(Y,\mathfrak{s}) \to HF^\infty(Y,\mathfrak{s})\right) \tag{3.4}$$

and

$$HF^{+}_{\mathsf{red}}(Y,\mathfrak{s}) := \operatorname{coker}\left(\pi_* : HF^\infty(Y,\mathfrak{s}) \to HF^+(Y,\mathfrak{s})\right). \tag{3.5}$$

The connecting homomorphism δ induces an isomorphism from $HF^{+}_{\mathsf{red}}(Y,\mathfrak{s})$ to $HF^{-}_{\mathsf{red}}(Y,\mathfrak{s})$. It is perhaps worth remarking that, unlike $HF^{\pm}$, the modules $HF^{\pm}_{\mathsf{red}}(Y,\mathfrak{s})$ are always finite-dimensional over $\mathbb{F}_2$.

3.2 Maps associated to cobordisms

Fix a four-dimensional cobordism W from Y_0 to Y_3, and let $\mathfrak{s}$ be a $Spin^c$-structure on W. Choose a self-indexing Morse function f on W. Then f decomposes W into a sequence of one-handle additions which taken together form a cobordism W_1, followed by some two-handle additions forming a cobordism W_2, and three-handle additions forming a cobordism W_3, in this order. Let Y_1 and Y_2 be the intermediate three-manifolds, so that

$$W = W_1 \cup_{Y_1} W_2 \cup_{Y_2} W_3.$$

Given this data, Ozsváth and Szabó [OS06] associate to $(W,\mathfrak{s})$ an induced map $F^\circ_{W,\mathfrak{s}} : HF^\circ(Y_0,\mathfrak{s}_{Y_0}) \to HF^\circ(Y_3,\mathfrak{s}_{Y_3})$ between the Floer homologies of Y_0 and Y_3 via the composition

$$F^\circ_{W,\mathfrak{s}} := F^\circ_{W_3,\mathfrak{s}|_{W_3}} \circ F^\circ_{W_2,\mathfrak{s}|_{W_2}} \circ F^\circ_{W_1,\mathfrak{s}|_{W_1}} \tag{3.1}$$

of maps associated to each of the pieces W_1, W_2, and W_3. We now review the definitions of these three maps.

One- and three-handle maps

Suppose that W_1 is a cobordism from Y_0 to Y_1 which consists entirely of 1-handle additions, and let $\mathfrak{s}$ be a $Spin^c$-structure on W_1. The map

$$F^{\circ}_{W_1,\mathfrak{s}} : HF^{\circ}(Y_0, \mathfrak{s}_{Y_0}) \to HF^{\circ}(Y_1, \mathfrak{s}_{Y_1})$$

is constructed in the following way. Denote the 1-handles by $h_1, \ldots, h_n$, and for each $i = 1, \ldots, n$ pick a path η_i in Y_0, which joins the two feet of the handle h_i. A choice of the η_i induces a connected sum decomposition $Y_1 \cong Y_0 \#(S^1 \times S^2)^{\# n}$ where the first homology of each $S^1 \times S^2$ factor is generated by the union of η_i with the core of the corresponding handle. Further, the restriction of $\mathfrak{s}$ to the $(S^1 \times S^2)$-summands in Y_1 is torsion. It follows that

$$HF^{\circ}(Y_1, \mathfrak{s}_{Y_1}) \cong HF^{\circ}(Y_0, \mathfrak{s}_{Y_0}) \otimes \Lambda^*(H_1(S^1 \times S^2))$$

Let Θ^+ be the generator of the top-graded part of $\Lambda^*(H_1(S^1 \times S^2))$. Then the Heegaard Floer map induced by W_1 is given by

$$F^{\circ}_{W_1,\mathfrak{s}}([\mathbf{x}, i]) = [\mathbf{x} \otimes \Theta^+, i] \tag{3.2}$$

It is proved in [OS06, Section 4.3] that, up to composition with canonical isomorphisms, $F^{\circ}_{W_1,\mathfrak{s}}$ does not depend on the choices made in its construction. For brevity, we will usually denote the 1-handle map by F_1.

Next, if W_3 is cobordism which can be built using only 3-handles, then for $\mathfrak{s} \in Spin^c(W)$ the map

$$F^\circ_{W_3,\mathfrak{s}} : HF^\circ(Y_2, \mathfrak{s}_{Y_2}) \to HF^\circ(Y_3, \mathfrak{s}_{Y_3})$$

is constructed in the following manner. After reversing W_3, we can view it as attaching 1-handles on Y_3 to get Y_2. Again, choose a collection of paths $\{\eta_i\}$ between the feet of these 1-handles in Y_3. Such a choice yields a decomposition $Y_2 \cong Y_3\#(\#^m S^1 \times S^2)$, where m is the number of 3-handles of W_3. Further, the restriction of $\mathfrak{s}$ to the $(S^1 \times S^2)$-summands in Y_2 is torsion. It follows that

$$HF^\circ(Y_2, \mathfrak{s}_{Y_2}) \cong HF^\circ(Y_3, \mathfrak{s}_{Y_3}) \otimes \Lambda^*(H_1(S^1 \times S^2))$$

Let Θ^- be the generator of the lowest-graded part of $\Lambda^*(H_1 \times S^2)$. Then the Heegaard Floer map induced by W_3 is given by

$$F^\circ_{W_3,\mathfrak{s}}([\mathbf{x} \otimes \Theta^-, i]) = [\mathbf{x}, i] \tag{3.3}$$

and

$$F^\circ_{W_3,\mathfrak{s}}([\mathbf{x} \otimes \boldsymbol{\xi}, i]) = 0$$

for any homogeneous generator $\boldsymbol{\xi}$ of $\Lambda^* H_1(S^1 \times S^2)$ not lying in the minimal degree. Again, the map is independent of the choices made in its construction.

Two-handle maps

In [OS06, Definition 4.2] Ozsváth and Szabó associate to a four-dimensional cobordism W consisting of two-handle additions certain kinds of triple Heegaard diagrams. The cobordism W from Y_1 to Y_2 corresponds to surgery on some framed link $\mathbb{L} \subset Y_1$. Denote by ℓ the number of components of $\mathbb{L}$. Fix a basepoint in Y_1. Let $B(\mathbb{L})$ be the union of $\mathbb{L}$ with a path from each component to the basepoint. The boundary of a regular neighborhood of $B(\mathbb{L})$ is a genus ℓ surface, which has a subset identified with ℓ punctured tori F_i, one for each link component.

Definition 3.1. A Heegaard triple $(\Sigma, \boldsymbol{\alpha}, \boldsymbol{\beta}, \boldsymbol{\gamma}, w)$ is called *subordinate to a bouqet* $B(\mathbb{L})$ if

(B1) $(\Sigma, \{\alpha_1, \dots, \alpha_g\}, \{\beta_1, \dots, \beta_{g-\ell}\})$ describes the complement of $B(\mathbb{L})$.

(B2) $\{\gamma_1, \dots, \gamma_{g-\ell}\}$, are small isotopic translates of $\{\beta_1, \dots, \beta_{g-\ell}\}$

(B3) After surgering out the $\{\beta_1, \dots, \beta_{g-\ell}\}$, the induced curves β_i and γ_i, for $i = g - \ell + 1, \dots, g$, lie on the punctured torus F_i.

(B4) For $i = g - \ell + 1, \dots, g$, the curves β_i represent meridians for the link components, disjoint from all γ_j for $i \neq j$, and meeting γ_i in a single transverse point.

(B5) for $i = g - \ell + 1, \dots, g$, the homology classes of the γ_i correspond to the framings of the link components.

The following lemma shows that one can represent the cobordism $W(\mathbb{L})$ via a Heegaard triple subordinate to a bouquet for the framed link $\mathbb{L}$. For a proof, see for example [Zem15, Lemma 9.4] or [OS06, Proposition 4.3].

Lemma 3.2. *Suppose* $(\Sigma, \alpha, \boldsymbol{\beta}, \boldsymbol{\gamma}, w)$ *is subordinate to a bouquet for a framed link* $\mathbb{L}$ *in* Y*. After filling in the boundary component* $Y_{\boldsymbol{\beta},\boldsymbol{\gamma}}$ *with* 3- *and* 4-*handles, we obtain the handle cobordism* $W(Y, \mathbb{L})$*.*

We now define the cobordism maps for 2-handle cobordisms. Suppose $\mathbb{L} \subset Y$ is a framed link in Y, and $B(\mathbb{L})$ is a bouquet. Let $(\Sigma, \boldsymbol{\alpha}, \boldsymbol{\beta}, \boldsymbol{\gamma}, w)$ be a Heegaard triple subordinate to $B(\mathbb{L})$. Let $\Theta \in \mathbb{T}_{\boldsymbol{\beta}} \cap \mathbb{T}_{\boldsymbol{\gamma}}$ denote the intersection point in top Maslov grading [OS06, Section 2.4].

If $\mathfrak{s} \in Spin^c(W(Y,\mathbb{L}))$, the 2-handle map

$$F^-_{\mathbb{L},\mathfrak{s}} : CF^-(\Sigma, \boldsymbol{\alpha}, \boldsymbol{\beta}, w, \mathfrak{s}|_Y) \to CF^-(\Sigma, \boldsymbol{\beta}, \boldsymbol{\gamma}, w, \mathfrak{s}|_{Y(\mathbb{L})})$$

is defined as a count of holomorphic triangles

$$F^-_{\mathbb{L},\mathfrak{s}}([\mathbf{x}, i]) := \sum_{\mathbf{y} \in \mathbb{T}_{\boldsymbol{\alpha}} \cap \mathbb{T}_{\boldsymbol{\gamma}}} \sum_{\substack{\psi \in \pi_2(\mathbf{x}, \Theta_{\beta,\boldsymbol{\gamma},\mathbf{y}} \\ \mu(\psi)=0 \\ s_w(\psi)=\mathfrak{s}}} \#\mathcal{M}(\psi) \cdot [i - n_w(\psi)], \tag{3.4}$$

where $\pi_2(\mathbf{x}, \Theta, \mathbf{y})$ is the set of homotopy classes of Whitney triangles with vertices $\mathbf{x}, \Theta, \mathbf{y}$, and $\mathcal{M}(\varphi)$ is the moduli space of holomorphic representatives of φ.

Throughout Section 4, we will be interested in studying the holomorphic triangle map (3.4) for diagrams which are not a priori subordinate to a bouquet for a framed link. We address this issue there.

Chapter 4

Trisections and Ozsváth-Szabó four-manifold invariants

In this section we demonstrate how one can use the data of a relative trisection map $\pi : X^4 \to \mathbb{R}^2$ to compute the cobordism maps of Ozsváth and Szabó.

4.1 A Mayer-Vietoris strategy

For a closed 4-manifold X with $b_2^+(X) \geq 2$ Ozsváth and Szabó defined a map

$$\Phi_X : Spin^c(X) \to \mathbb{F}_2$$

It is common to write $\Phi_{X,\mathfrak{s}}$ for the value of Φ_X on $\mathfrak{s}$. The map Φ_X is referred to as the *mixed invariant* of X, because it intertwines HF^+ and HF^-.

The map Φ_X is defined by picking a connected, codimension one submanifold $N \subset X$ that cuts X into two pieces, W_1 and W_2, such that $b_2^+(W_i) > 0$, and such that the restriction map

$$H^2(X) \to H^2(W_1) \oplus H^2(W_2)$$

is an injection. Such a three-manifold N is called an *admissible cut*. If we view W_1 as a cobordism from S^3 to N, and W_2 as a cobordism from N to S^3 the maps $F^\infty_{W_1,\mathfrak{s}|_{W_1}}$ and $F^\infty_{W_2,\mathfrak{s}|_{W_2}}$ vanish [OS06, Lemma 8.2]. Consequently, the image of $F^-_{W_1,\mathfrak{s}|_{W_1}}$ lands in $HF^-_{\mathsf{red}}(N,\mathfrak{s}|_N)$ and the map $F^+_{W_2,\mathfrak{s}|_{W_2}}$ factors through $HF^+_{\mathsf{red}}(N,\mathfrak{s}|_N)$. Finally, using the isomorphism between $HF^-_{\mathsf{red}}(N,\mathfrak{s}|_N)$ and $HF^+_{\mathsf{red}}(N,\mathfrak{s}|_N)$ via δ, one arrives at the following diagram

$$\begin{array}{ccccccc} & & & & & & HF^-(S^3) \\ & & & & & \swarrow & \downarrow F^-_{W_1,\mathfrak{s}|_{W_1}} \\ HF^+(N,\mathfrak{s}|_N) & \longrightarrow & HF^+_{\mathsf{red}}(N,\mathfrak{s}|_N) & \xrightarrow{\delta} & HF^-_{\mathsf{red}}(N,\mathfrak{s}|_N) & \longrightarrow & HF^-(N,\mathfrak{s}|_N) \\ F^+_{W_2,\mathfrak{s}|_{W_2}} \downarrow & \swarrow & & & & & \\ HF^+(S^3) & & & & & & \end{array}$$

Recall that the Floer homology groups of S^3 can be computed as

$$HF^-_k(S^3) = \begin{cases} \mathbb{F}_2 & \text{if } k \text{ is even and } k \leq -2 \\ 0 & \text{else} \end{cases} \qquad HF^+_k(S^3) = \begin{cases} \mathbb{F}_2 & \text{if } k \text{ is even and } k \geq 0 \\ 0 & \text{else} \end{cases}$$

The invariant $\Phi_{X,\mathfrak{s}}$ is defined as the coefficient of the bottom-graded generator Θ_+ of $HF^+_{(0)}(S^3)$ in the expression

$$\left(F^+_{W_2,\mathfrak{s}|_{W_2}} \circ \delta^{-1} \circ F^-_{W_1,\mathfrak{s}|W_1}\right)(\Theta_-) \tag{4.1}$$

where Θ_- denotes the top-graded generator of $HF^-_{(-2)}(S^3) \cong \mathbb{F}_2$. Ozsváth and Szabó prove that this is independent of the choices made (for example, the choice of admissable cut).

An equivalent formulation is to utilize the pairing on Heegaard Floer homology defined on $CF^\infty(Y,w,\mathfrak{s})$ via

$$\langle\cdot,\cdot\rangle : CF^\infty(Y,w,\mathfrak{s}) \otimes CF^\infty(-Y,w,\bar{\mathfrak{s}}) \to \mathbb{F}_2 \qquad \langle[\mathbf{x},i],[\mathbf{y},j]\rangle = \begin{cases} 1 & \text{if } i+j=-1 \text{ and } \mathbf{x}=\mathbf{y} \\ 0 & \text{else} \end{cases} \tag{4.2}$$

This pairing descends to one on $\langle\cdot,\cdot\rangle : HF^+_{\mathsf{red}}(Y,w,\mathfrak{s}) \otimes HF^-_{\mathsf{red}}(-Y,w,\bar{\mathfrak{s}}) \to \mathbb{F}_2$ [OS06, Section 5.1]. Using this pairing, we can alternatively define $\Phi_{X,\mathfrak{s}}$ via the duality properties of Heegaard Floer homology. Namely, instead of viewing W_2 as a cobordism from N to S^3, we can 'turn W_2 around', and view it as a cobordism $\overline{W}_2 : -S^3 \to -N$, where $-N$ denotes the three-manifold N with its orientation reversed. In [OS06, Section 5.1], Ozsváth and Szabó show that the maps

$$F^-_{\overline{W}_2,\bar{\mathfrak{s}}} \qquad \text{and} \qquad F^+_{W_2,\mathfrak{s}}$$

are adjoint to each other with respect to $\langle\cdot,\cdot\rangle$.

Following [JM08], we make the following definition.

Definition 4.1. For a smooth, compact, connected, oriented *Spin*^{c} four-manifold $(W,\mathfrak{s})$ with connected boundary $\partial W = Y$, we define the *relative invariant* of $(W,\mathfrak{s})$ to be the image of $\Theta_- \in HF^-_{(-2)}(S^3)$ under the cobordism map where we view W as a cobordism from

$$\begin{array}{ccc} HF^-(S^3) & \xrightarrow{F^-_{W,\mathfrak{s}}} & HF^-(Y,\mathfrak{s}|_Y) \\ \Theta_- & \longmapsto & \Psi_{W,\mathfrak{s}} \end{array}$$

S^3 to Y after removing a small four-ball from W.

It follows from the discussion above that if X is a four-manifold with $b_2^+(X) \geq 2$ and is decomposed into two pieces as above, then the mixed invariants can be recovered as

$$\Phi_{X,\mathfrak{s}} = \langle \delta^{-1}\Psi_{W_1,\mathfrak{s}|W_1}, \Psi_{\overline{W}_2,\bar{\mathfrak{s}}|_{\overline{W}_2}} \rangle \tag{4.3}$$

With this strategy in mind, our main focus in the upcoming sections will be on computing the relative invariants from a (relative) trisection.

4.2 Constructing Heegaard triples from relative trisection diagrams

Fix X^4 to be a compact, oriented, connected, smooth 4-manifold. The input data we require is a tuple $(\pi, g, \mathcal{H})$ consisting of a $(g, k; p, b)$-trisection map $\pi : X \to \mathbb{R}^2$, a Riemannian metric g on X, and a π-compatible connection $\mathcal{H}$. Equipped with such data, we may choose three reference arcs $\eta_{\boldsymbol{\alpha}}, \eta_{\boldsymbol{\beta}}, \eta_{\boldsymbol{\gamma}} : [0, 1] \to \mathbb{R}^2$ as in Figure 4.1 below. Associated to these reference

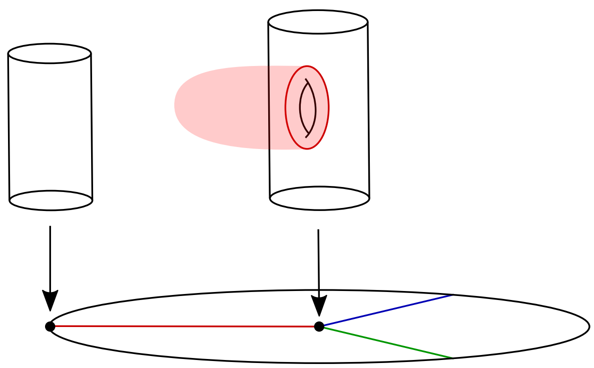

Figure 4.1: For $\boldsymbol{\tau} \in \{\boldsymbol{\alpha}, \boldsymbol{\beta}, \boldsymbol{\gamma}\}$, we have reference arcs $\eta_{\boldsymbol{\tau}} : [0, 1] \to \mathbb{R}^2$ for which $f_{\boldsymbol{\tau}} : U_{\boldsymbol{\tau}} \to [0, 3]$ is a Morse function.

arcs are three Morse functions $f_{\boldsymbol{\alpha}}, f_{\boldsymbol{\beta}}, f_{\boldsymbol{\gamma}}$ defined on the compression bodies $U_{\boldsymbol{\alpha}}, U_{\boldsymbol{\beta}}$, and $U_{\boldsymbol{\gamma}}$ respectively. For $\boldsymbol{\tau} \in \{\boldsymbol{\alpha}, \boldsymbol{\beta}, \boldsymbol{\gamma}\}$, these Morse functions satisfy:

- $f_{\boldsymbol{\tau}} : U_{\boldsymbol{\tau}} \to [0, 3]$ is a Morse function with $f_{\boldsymbol{\tau}}^{-1}(0) = \Sigma$ and $f_{\boldsymbol{\tau}}^{-1}(3) = \Sigma_{\boldsymbol{\tau}}$ the surface obtained by doing surgery on Σ along the $\boldsymbol{\tau}$-curves; and,
- $f_{\boldsymbol{\tau}}$ has $g - p$ index two critical points whose descending manifolds intersect Σ along the $\boldsymbol{\tau}$ curves.

We define the surface $\Sigma_{\boldsymbol{\alpha}}$ to be the fiber $f_{\boldsymbol{\alpha}}^{-1}(3)$ and fix an identification $\Sigma_{\boldsymbol{\alpha}} \cong \Sigma_{p,b}$. Next, endow $\Sigma_{\boldsymbol{\alpha}}$ with a model collection of pairwise disjoint arcs $\{a_1, \ldots, a_n\}$ which constitute a basis for $H_1(\Sigma_{\boldsymbol{\alpha}}; \partial\Sigma_{\boldsymbol{\alpha}})$, as in Figure 4.2 below. We call such a collection the *standard arc basis*, and note that n can be computed as $n = 2p + b - 1$.

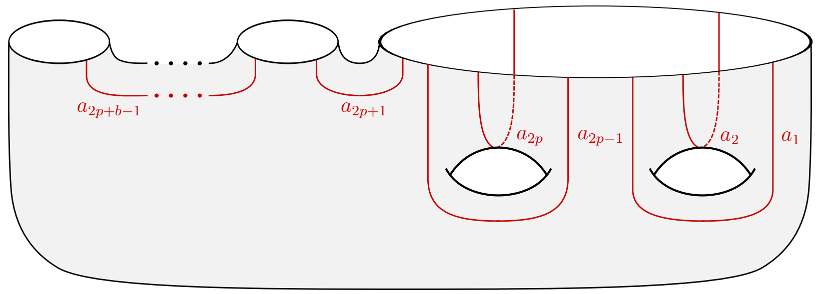

Figure 4.2: The standard arc basis of $H_1(\Sigma_{\boldsymbol{\alpha}}, \partial\Sigma_{\boldsymbol{\alpha}} l\mathbb{Z})$.

Now define $\{b_1, \ldots, b_n\} \subset \Sigma_{\boldsymbol{\alpha}}$ and $\{c_1, \ldots, c_n\} \subset \Sigma_{\boldsymbol{\alpha}}$ to be two additional arc bases which satisfy the following conditions:

1. The arc bases $\{a_1, \ldots, a_n\}$, $\{b_1, \ldots, b_n\}$ and $\{c_1, \ldots, c_n\}$ are isotopic (not relative to the endpoints) by a small isotopy;

2. For each $i = 1, \ldots, n$, a_i has a single positive transverse intersection with b_i, where the orientation of b_i is inherited from a_i.

3. For each $i = 1, \ldots, n$, b_i has a single positive transverse intersection with c_i, where the orientation of the c_i is inherited from the b_i.

4. For each $i = 1, \ldots, n$, a_i has a single positive intersection with c_i.

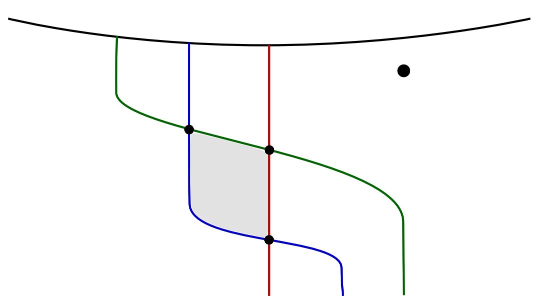

Figure 4.3: A zoomed in picture near the boundary of $\Sigma_{\boldsymbol{\alpha}}$.

Next, we can flow the arcs $\{a_1, \ldots, a_n\} \subset \Sigma_{\boldsymbol{\alpha}}$ onto Σ using the gradient flow of $f_{\boldsymbol{\alpha}}$. We'll denote the images of $\{a_1, \ldots, a_n\}$ under this flow by $\{\mathfrak{a}_1, \ldots, \mathfrak{a}_n\} \subset \Sigma$. Note that generic choices ensure that the $\mathfrak{a}_i$ are pairwise disjoint form each other and from the original $\boldsymbol{\alpha}$-curves

$\{\boldsymbol{\alpha}_1, \ldots, \boldsymbol{\alpha}_{g-p}\} \subset \Sigma$. Note, however, that the images $\{\mathfrak{a}_1, \ldots, \mathfrak{a}_n\}$ are only well-defined up to handle-slides over the original $\boldsymbol{\alpha}$-curves.

Now, perform a sequence of handle-slides of $\mathfrak{a}$ arcs over $\boldsymbol{\alpha}$ curves until $\mathfrak{a} \cap \boldsymbol{\beta} = \emptyset$, and denote the resulting collection of arcs by $\mathfrak{b} = \{\mathfrak{b}_1, \ldots, \mathfrak{b}_n\}$. Note that this construction of the collection $\mathfrak{b}$ is equivalent to the following. According to [CGP18, Corollary 14], there exists an 'identity' map $\mathsf{id}_{\boldsymbol{\alpha}\boldsymbol{\beta}} : \Sigma_{\boldsymbol{\alpha}} \to \Sigma_{\boldsymbol{\beta}}$ for which the following diagram commutes

$$\begin{array}{ccc} \Sigma_{\boldsymbol{\alpha}} & & \\ {\scriptstyle \mathsf{id}_{\boldsymbol{\alpha},\boldsymbol{\beta}}}\big\downarrow & \searrow^{\nabla f_{\boldsymbol{\alpha}}} & \\ \Sigma_{\boldsymbol{\beta}} & \xrightarrow[\nabla f_{\boldsymbol{\beta}}]{} & \Sigma \end{array}$$

Finally, perform another sequence of arcslides of $\mathfrak{b}$ arcs over $\boldsymbol{\beta}$ curves until $\mathfrak{b} \cap \boldsymbol{\gamma} = \emptyset$, and denote the resulting collection of arcs by $\mathfrak{c} = \{\mathfrak{c}_1, \ldots, \mathfrak{c}_n\}$. By construction, the data $\mathfrak{D} = (\Sigma, \boldsymbol{\alpha}, \boldsymbol{\beta}, \boldsymbol{\gamma}; \mathfrak{a}, \mathfrak{b}, \mathfrak{c})$ constitute an arced trisection diagram of X.

We now describe how to glue together the above data to construct a Heegaard triple which encodes the cobordism $X : \emptyset \to Y$. Let $\underline{\Sigma}$ be the surface obtained by identifying the boundaries of Σ and $-\Sigma_{\boldsymbol{\alpha}}$ via an orientation reversing diffeomorphism

$$\underline{\Sigma} := \Sigma \cup_\partial -\Sigma_{\boldsymbol{\alpha}}. \tag{4.1}$$

Note that the genus of $\underline{\Sigma}$ is $g(\underline{\Sigma}) = g + p + b - 1$.

Next, we define three new handlebodies $U_{\underline{\boldsymbol{\alpha}}}, U_{\underline{\boldsymbol{\beta}}}$, and $U_{\underline{\boldsymbol{\gamma}}}$, each bounded by $\underline{\Sigma}$, by specifying their attaching curves. The $U_{\underline{\boldsymbol{\alpha}}}$ handlebody is determined by the curves $\{\underline{\boldsymbol{\alpha}}_1, \ldots, \underline{\boldsymbol{\alpha}}_{g+p+b-1}\}$ where

$$\underline{\boldsymbol{\alpha}}_i = \begin{cases} \alpha_i & 1 \le i \le |\boldsymbol{\alpha}| \\ \mathfrak{a}_i \cup_\partial \overline{a}_i & |\boldsymbol{\alpha}| + 1 \le i \le g(\underline{\Sigma}) \end{cases} \tag{4.2}$$

For the $\underline{\boldsymbol{\beta}}$-handlebody $U_{\underline{\boldsymbol{\beta}}}$, we define

$$\underline{\boldsymbol{\beta}}_i = \begin{cases} \beta_i & 1 \leq i \leq |\boldsymbol{\beta}| \\ \mathfrak{b}_i \cup_\partial \overline{b}_i & |\boldsymbol{\beta}| + 1 \leq i \leq g(\underline{\Sigma}) \end{cases} \tag{4.3}$$

Finally, the $\underline{\boldsymbol{\gamma}}$-handlebody $U_{\underline{\boldsymbol{\gamma}}}$ is determined by

$$\underline{\boldsymbol{\gamma}}_i = \begin{cases} \boldsymbol{\gamma}_i & 1 \leq i \leq |\boldsymbol{\gamma}| \\ \mathfrak{c}_i \cup_\partial \overline{c}_i & |\boldsymbol{\gamma}| + 1 \leq i \leq g(\underline{\Sigma}) \end{cases} \tag{4.4}$$

Example 4.2. Consider for example the standard relative trisection diagram for B^4. After this procedure, the resulting Heegaard triple looks like Figure below.

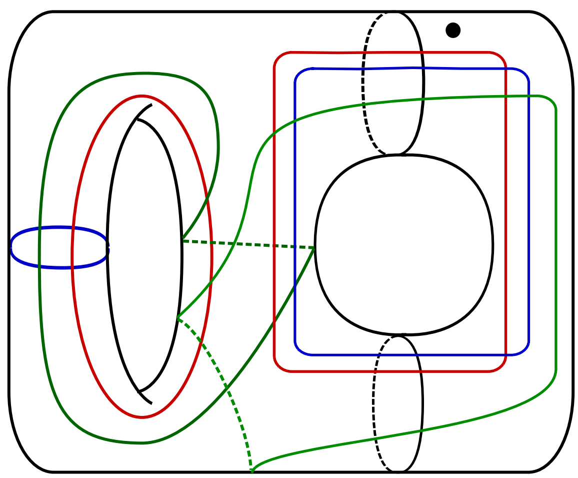

Figure 4.4: A Heegaard triple constructed from the relative trisection diagram for B^4.

Thus far, we have described how, given a relative trisection diagram $\mathfrak{D} = (\Sigma, \boldsymbol{\alpha}, \boldsymbol{\beta}, \boldsymbol{\gamma})$ which is compatible with a given $(g, k; p, b)$-trisection map $f : X \to \mathbb{D}^2$, to construct a new Heegaard triple $\underline{\mathfrak{D}} = (\underline{\Sigma}, \underline{\boldsymbol{\alpha}}, \underline{\boldsymbol{\beta}}, \underline{\boldsymbol{\gamma}})$. However, it is not at all clear how the original 4-manifold X, as described by the diagram $\mathfrak{D}$, and the potentially new 4-manifold $\underline{X}$, as described by the diagram $\underline{\mathfrak{D}}$, are related. The remainder of this section clarifies this relationship via a technique which we call a *trisector's cut*.

Our strategy for relating X and $\underline{X}$ involves a series of intermediate manifolds which we now describe. Starting with X, which comes equipped with the decomposition $X = X_1 \cup X_2 \cup X_3$, consider a collar neighborhood of the boundary of X_3, denoted $\nu(\partial X_3)$. After rounding corners we parametrize this collar neighborhood via

$$\varphi : [0,1] \times \#^{k_3} S^1 \times S^2 \to \nu(\partial X_3),$$

where ∂X_3 is embedded in $\nu(\partial X_3)$ as $\{0\} \times \#^{k_3} S^1 \times S^2$. For a chosen basepoint $z \in f^{-1}(1) \cong P$, let

$$\eta : [0,1] \to \nu(\partial X_3)$$

be a short arc connecting z to its image in $\{1\} \times f^{-1}(1)$. This being done, delete from X_3 the complement of $\nu(\partial X_3)$ union a tubular neighborhood of η. In symbols, delete the following subset from X_3:

$$\big(X_3 \setminus \nu(\partial X_3)\big) \cup \nu(\eta) \tag{4.5}$$

We give the resulting 4-manifold a name, $X^{\#}$, and its importance is demonstrated in Proposition 4.3 below.

Proposition 4.3. *The* 4*-manifolds* $X^{\#}$ *and* $\underline{X}$ *are diffeomorphic, where* $\underline{X}$ *is the result of filling in* $X_{\underline{\boldsymbol{\alpha}},\underline{\boldsymbol{\beta}},\underline{\boldsymbol{\gamma}}}$ *with* $k_2 + 2p + b - 1$ 3*-handles and a single* 4*-handle.*

Remark 2. The author would like to warmly thank David Gay and Juanita Pinzón-Caicedo for helpful suggestions during the development of this proof.

Proof. The essential point of the argument is showing how to embed the spine of $\underline{X}$ into $X^{\#}$. To do so, we need to identify the central surface $\underline{\Sigma}$ and the corresponding handlebodies $U_{\underline{\boldsymbol{\alpha}}}, U_{\underline{\boldsymbol{\beta}}}$, and $U_{\underline{\boldsymbol{\gamma}}}$ as submanifolds of $X^{\#}$. The result then follows after filling in the resulting $\#^{\ell_i} S^1 \times S^2$ with $\natural^{\ell_i} S^1 \times B^3$ where ℓ_i, $i = 1, 2, 3$, are parameters to be determined.

Observe that, after removing $\natural^{k_3} S^1 \times B^3$ from $X_3 \subset X$, the base diagram is now reminiscent of the familiar *keyhole* contour which we parametrize as $B = [\pi/6, 11\pi/6] \times [0, 1]$ where $\theta \in [\pi/6, 11\pi/6]$ and $t \in [0, 1]$ are coordinates.

We say that a parametrization $\kappa : B \to [\pi/6, 11\pi/6] \times [0, 1]$ is *compatible with* f if the critical image $C_\kappa := \kappa \circ f(\mathsf{Crit}(f))$ is in the following standard position:

- All cusps point to the right (i.e. in the positive t-direction).
- Each $R_\theta := \{\theta\} \times [0, 1]$ meets C_κ in exactly $g - p$ points, and each intersection is either at a cusp or meets transversely in a fold point.
- For a fixed small $\varepsilon > 0$, there exists a 2ε-neighborhood $N_{2\varepsilon}$ of $\partial^\theta B := [\pi/6, 11\pi/6] \times \{0, 1\}$ such that $\kappa \circ f(\mathsf{Crit}(f)) \cap N_{2\varepsilon} = \emptyset$.

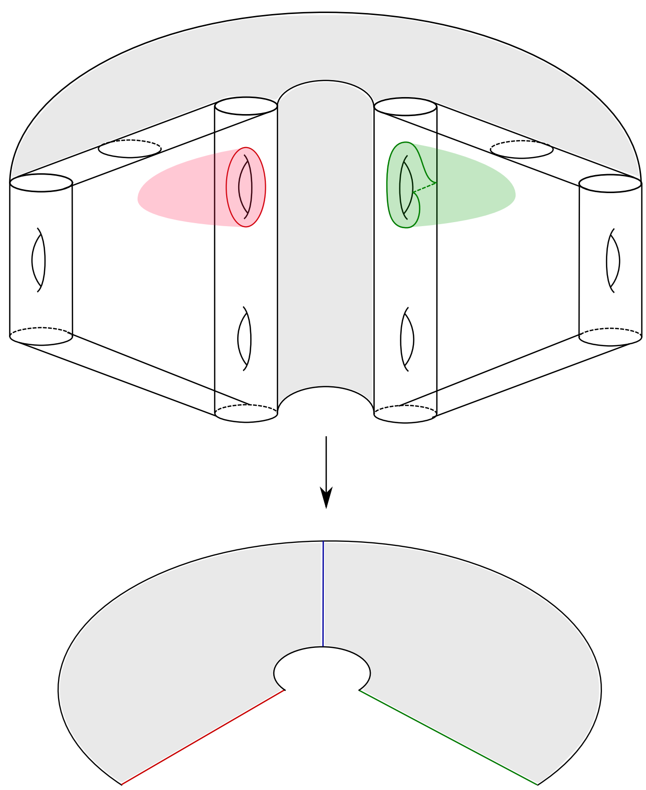

Figure 4.5: The trisector's cut.

Fix an f-compatible parametrization $\kappa : B \to [\pi/6, 11\pi/6] \times [0,1]$ of the base, and consider the reference arcs $R_{\boldsymbol{\alpha}} := \{-\pi/3\} \times [0,1]$, $R_{\boldsymbol{\beta}} := \{\pi\} \times [0,1]$, and $R_{\boldsymbol{\gamma}} := \{\pi/3\} \times [0,1]$. Observe that

$$H_{\underline{\boldsymbol{\alpha}}} := f^{-1}(R_{\boldsymbol{\alpha}})$$
$$H_{\underline{\boldsymbol{\beta}}} := f^{-1}(R_{\boldsymbol{\beta}})$$
$$H_{\underline{\boldsymbol{\gamma}}} := f^{-1}(R_{\boldsymbol{\gamma}})$$

are each sutured compression bodies. Next, we'll round the corners of these compression bodies and obtain honest 3-dimensional handlebodies. For a proof, see [JZ18b, Lemma 8.4].

Lemma 4.4. *Let $H_{\boldsymbol{\alpha}}$ be the sutured compression body formed by attaching 3-dimensional 2-handles to $I \times \Sigma$ along the curves $\{0\} \times \boldsymbol{\alpha}$. After rounding corners, we can view $U_{\boldsymbol{\alpha}}$ as a (non-sutured) handlebody of genus $|\boldsymbol{\alpha}| - \chi(R_{\boldsymbol{\alpha}}) + 1$ and boundary*

$$\big(\{1\} \times \Sigma\big) \cup_\partial \overline{\Sigma}_{\boldsymbol{\alpha}}.$$

Furthermore, a set of compressing disks for $U_{\boldsymbol{\alpha}}$ can be obtained by taking $|\boldsymbol{\alpha}|$ compressing disks $D_{\boldsymbol{\alpha}}$ with boundary $\{1\} \times \boldsymbol{\alpha}$ for $\alpha \in \boldsymbol{\alpha}$, as well as disks of the form $D_{c_i^*} := I \times c_i^*$ for pairwise disjoint, embedded arcs $c_1^*, \ldots, c_{b_1 \Sigma_{\boldsymbol{\alpha}}}^*$ in Σ that avoid the $\boldsymbol{\alpha}$ curves, and form a basis of $H_1(\Sigma_{\boldsymbol{\alpha}}, \partial \Sigma_{\boldsymbol{\alpha}})$. These cut $U_{\boldsymbol{\alpha}}$ into a single 3-ball.

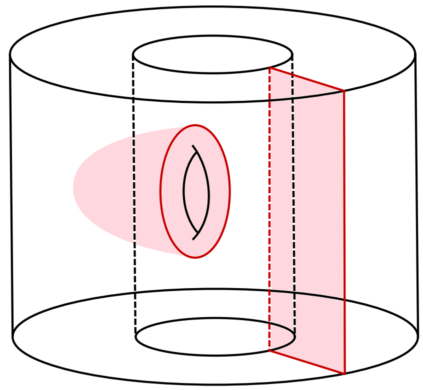

Figure 4.6: The process of rounding corners.

Applying Lemma 4.4 to the three sutured compression bodies $H_{\underline{\boldsymbol{\alpha}}}, H_{\underline{\boldsymbol{\beta}}}$, and $H_{\underline{\boldsymbol{\gamma}}}$ above, we obtain 3 three-dimensional handlebodies with $\partial H_{\boldsymbol{\tau}} = \underline{\Sigma}_{\boldsymbol{\tau}}$ for each $\boldsymbol{\tau} \in \{\underline{\boldsymbol{\alpha}}, \underline{\boldsymbol{\beta}}, \underline{\boldsymbol{\gamma}}\}$. We take as the central surface in our spine-decomposition of $X^{\#}$ to be $\underline{\Sigma} := \partial \underline{\Sigma}_{\underline{\boldsymbol{\alpha}}}$. Clearly, $\underline{\Sigma}$ bounds the $U_{\underline{\boldsymbol{\alpha}}}$ handle-body described in equation (4.2). Notice, however, that the $H_{\underline{\boldsymbol{\beta}}}$ and $H_{\underline{\boldsymbol{\gamma}}}$ handlebodies are completely disjoint from $\underline{\Sigma}$. To remedy this, we isotope the attaching circles for the $\underline{\boldsymbol{\beta}}$- and $\underline{\boldsymbol{\gamma}}$-handlebodies onto $\underline{\Sigma}$, and it is via this isotopy that we see how the monodromy of the open book decomposition of Y naturally arises. After isotoping the attaching curves onto the same central surface $\underline{\Sigma}$, we will have completed the proof that the spine of $X_{\underline{\boldsymbol{\alpha}},\underline{\boldsymbol{\beta}},\underline{\boldsymbol{\gamma}}}$ embeds into $X^{\#}$.

Now, we'll construct an isotopy for the attaching circles for the handlebodies $U_{\underline{\boldsymbol{\beta}}}$ and $U_{\underline{\boldsymbol{\gamma}}}$. To do so, choose a connection $\mathcal{H}$ for the trisection map f, and thicken the surface $\underline{\Sigma}_{\boldsymbol{\beta}}$ to $\underline{\Sigma}_{\boldsymbol{\beta}} \times [0, 2\varepsilon]$ using the inward pointing normal direction coming from the boundary. Since we have an f-compatible parametrization of the base, the attaching circles on $\underline{\Sigma}_{\boldsymbol{\beta}} \times \{2\varepsilon\}$ are isotopic to those of $\underline{\Sigma}_{\underline{\boldsymbol{\beta}}} = \underline{\Sigma}_{\underline{\boldsymbol{\beta}}} \times \{0\}$. Next, we use $\mathcal{H}$ to flow the attaching circles on $\underline{\Sigma}_{\underline{\boldsymbol{\beta}}} \times \{2\varepsilon\}$ onto to $\underline{\Sigma}_{\boldsymbol{\alpha}} \times \{2\varepsilon\}$. Finally, we see that the attaching curves for $H_{\underline{\boldsymbol{\beta}}}$, appropriately isotoped over to $\underline{\Sigma}$, are precisely those for $U_{\underline{\boldsymbol{\beta}}}$. With the attaching circles for $U_{\underline{\boldsymbol{\beta}}}$ pushed slightly in, it follows by the horizontality condition that the attaching circles for $H_{\underline{\boldsymbol{\gamma}}}$, after flowing along the horizontal distribution, agree with that of $U_{\underline{\gamma}}$. Thus, we have shown that the spine of $X_{\underline{\alpha},\underline{\beta},\underline{\gamma}}$ embeds into $X^{\#}$.

It remains only to show that after filling in the caverns, one gets $X^{\#}$ back, but this follows from uniqueness of [LP72]. $\square$

Remark 3. The boundary of $X^{\#}$ is $Y\#(\#^{k_3}S^1 \times S^2)$, and after filling in the $\#^{k_3}S^1 \times S^2$, we recover the original 4-manifold X.

Corollary 4.5. *In the Heegaard triple $(\underline{\Sigma}, \underline{\boldsymbol{\alpha}}, \underline{\boldsymbol{\beta}}, \underline{\boldsymbol{\gamma}}, w)$ constructed above, we have that $(\underline{\Sigma}, \underline{\boldsymbol{\alpha}}, \underline{\boldsymbol{\beta}})$, $(\underline{\Sigma}, \underline{\boldsymbol{\beta}}, \underline{\boldsymbol{\gamma}})$ and $(\underline{\Sigma}, \underline{\boldsymbol{\alpha}}, \underline{\boldsymbol{\gamma}})$ are Heegaard diagrams for the three-manifolds $\#^{\ell_1}S^1 \times S^2$, $\#^{\ell_2}S^1 \times S^2$, and $Y\#(\#^{k_3}S^1 \times S^2)$ where $\ell_i = k_i + 2p + b - 1$.*

Proof. The statements for $(\underline{\Sigma}, \underline{\boldsymbol{\alpha}}, \underline{\boldsymbol{\beta}})$ and $(\underline{\Sigma}, \underline{\boldsymbol{\beta}}, \underline{\boldsymbol{\gamma}})$ follow from a combination of two facts; the first being that $(\Sigma, \boldsymbol{\alpha}, \boldsymbol{\beta}, \boldsymbol{\gamma})$ is a relative trisection, so that to begin with the pairwise tuples yield connect sums of $S^1 \times S^2$; and the second being that the monodromy of the open book can be trivialized over one sector at a time. $\square$

4.3 Holomorphic triangles and cobordism maps

Fix X to be a smooth, oriented, compact four-manifold with connected boundary, and equip X with a $(g, k; p.b)$-trisection map $\pi : X \to \mathbb{D}^2$. Given a diagram $(\Sigma, \boldsymbol{\alpha}, \boldsymbol{\beta}, \boldsymbol{\gamma})$ associated to π, we show in this section how the holomorphic triangle map (3.4) computes the induced cobordism map of Ozsváth and Szabó.

Proposition 4.6. *If $\underline{\mathcal{H}} = (\underline{\Sigma}, \underline{\boldsymbol{\alpha}}, \underline{\boldsymbol{\beta}}, \underline{\boldsymbol{\gamma}}, w)$ is a pointed Heegaard triple constructed using the prescription described in subsection 4.2 above, then $\underline{\mathcal{H}}$ is slide-equivalent to one which is subordinate to a bouquet for a framed link $\mathbb{L} \subset \#^{\ell_1}S^1 \times S^2$ for which the 2-handle cobordism $W(\#^{\ell_1}S^1 \times S^2, \mathbb{L})$ is diffeomorphic to $\underline{X}$ as cobordisms from $\#^{\ell_1}S^1 \times S^2$ to $Y^{\#}$, where $\underline{X}$ is the result of filling in $X_{\underline{\alpha},\underline{\beta},\underline{\gamma}}$ with $\natural^{\ell_2}S^1 \times B^3$ and a 4-handle.*

Proof. Consider again the singular fibration $\pi^\# : X^\# \to \mathbb{D}^2$ shown in Figure 4.5 along with the three reference arcs $\eta_{\boldsymbol{\alpha}}, \eta_{\boldsymbol{\beta}}$, and $\eta_{\boldsymbol{\gamma}}$ shown there. Choose an isotopy of the $\eta_{\boldsymbol{\alpha}}$ and $\eta_{\boldsymbol{\beta}}$ reference arcs, relative to the endpoints, so that they appear as in Figure 4.7 below.

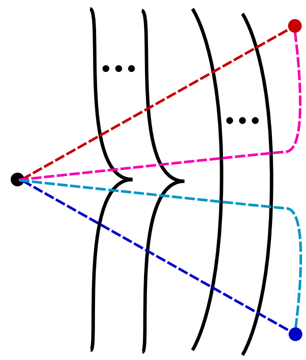

Figure 4.7: An isotopy of the $\eta_{\boldsymbol{\alpha}}$ and $\eta_{\boldsymbol{\beta}}$ reference arcs keeping the endpoints fixed.

During the chosen isotopy of $\eta_{\boldsymbol{\alpha}}$ and $\eta_{\boldsymbol{\beta}}$ the cut systems $\underline{\boldsymbol{\alpha}}$ and $\underline{\boldsymbol{\beta}}$ will evolve via a sequence of handleslides and the resulting diagram will have $\underline{\boldsymbol{\alpha}}'$ and $\underline{\boldsymbol{\beta}}'$ be in standard position with respect to on another.

Recall from [MSZ16, Definition 4.5] that a disk D_γ properly embedded in $U_{\underline{\boldsymbol{\gamma}}}$ is *primitive in $U_{\underline{\boldsymbol{\gamma}}}$ with respect to $U_{\underline{\boldsymbol{\beta}}'}$* if there exists a compression disk $D_{\beta_i'}$ satisfying the condition $|D_\gamma \cap D_{\beta_i'}| = 1$. Since $(\Sigma, \underline{\boldsymbol{\beta}}', \underline{\boldsymbol{\gamma}})$ is a genus $\underline{g} = g+p+b-1$ Heegaard diagram for $\#^{\ell_2} S^1 \times S^2$, it follows from [MSZ16, Theorem 2.7] that $U_{\underline{\boldsymbol{\gamma}}}$ admits an ordered collection of compression disks $\{D_{\underline{\gamma}_i'}\}$ where the corresponding attaching circles $\underline{\gamma}_i' = \partial D_{\underline{\gamma}_i'}$ satisfy

1. For $i = 1, \ldots, g-k-p$, $\underline{\gamma}_i'$ satisfies $|\underline{\gamma}_i' \cap \underline{\boldsymbol{\beta}}_i'| = 1$ and $|\underline{\gamma}_i' \cap \underline{\boldsymbol{\beta}}_j| = 0$ for $i \neq j$.

2. For $i = g-k-p+1, \ldots, g+p+b-1$, $\underline{\gamma}_i'$ is parallel to $\underline{\boldsymbol{\beta}}_i'$.

We remark that since $\underline{\boldsymbol{\gamma}}'$ and $\underline{\boldsymbol{\gamma}}$ are cut systems for the same handlebody $U_{\underline{\boldsymbol{\gamma}}}$, it follows from [Joh06] that $\underline{\boldsymbol{\gamma}} \sim \underline{\boldsymbol{\gamma}}'$.

This being done, it follows from [KM20, p.5] (see, in particular [KM20, Figure 2]) that for $i = 1, \ldots, g-k-p$, $\underline{\gamma}_i'$ can be interpreted as the framed attaching sphere for a 2-handle cobordism, where each $\underline{\gamma}_i'$ is given the surface framing.

Finally, we exhibit a bouquet for the framed attaching link $\mathbb{L} = \{\underline{\gamma}'_1, \ldots, \underline{\gamma}'_{g-p-k}\}$ and check that $(\underline{\Sigma}, \underline{\boldsymbol{\alpha}}', \underline{\boldsymbol{\beta}}', \underline{\boldsymbol{\gamma}}')$ is subordinate to it. For each $\underline{\gamma}'_i \in \{\underline{\gamma}'_1, \ldots, \underline{\gamma}'_{g-k-p}\}$, choose a properly embedded arc $\eta_i \subset U_{\underline{\boldsymbol{\beta}}}$ which has one endpoint on $\underline{\gamma}'_i$ and the other on w, the fixed basepoint. Then the union of η_i comprise a bouquet for the link $\mathbb{L}$. Furthermore, $(\underline{\Sigma}, \{\underline{\boldsymbol{\alpha}}_1, \ldots, \underline{\boldsymbol{\alpha}}'_{g+p+b-1}\}, \{\underline{\boldsymbol{\beta}}'_{g-p-k+1}, \ldots, \underline{\boldsymbol{\beta}}'_{g+p+b-1}\}$ is a Heegaard diagram for the complement of $\mathbb{L}$ in $\#^{\ell_1} S^1 \times S^2$. Next, taking a thin tubular neighborhood of $\underline{\boldsymbol{\beta}}'_i \cup \underline{\gamma}'_i$ constitutes a punctured torus for each $i = 1, \ldots, g-k-p$. Last, the conditions that $\underline{\boldsymbol{\beta}}'_i$ constitute a meridian and that $\underline{\gamma}'_i$ constitute a longitude are self evident after using the surface framing to push $\underline{\gamma}'_i$ into $U_{\underline{\boldsymbol{\beta}}}$ handlebody. Thus, the conditions **(B1)** – **(B5)** are satisfied. □

Definition 4.7. Let $(\Sigma, \boldsymbol{\alpha}, \boldsymbol{\beta}, \boldsymbol{\gamma})$ be an admissable triple diagram. If $\boldsymbol{\beta} \sim \boldsymbol{\gamma}$, then we'll write $\Psi^{\boldsymbol{\alpha}}_{\boldsymbol{\beta} \to \boldsymbol{\gamma}}$ for the map

$$F^\circ_{\boldsymbol{\alpha},\boldsymbol{\beta},\boldsymbol{\gamma}}(- \otimes \Theta_{\boldsymbol{\beta},\boldsymbol{\gamma}}) : HF^\circ(\Sigma, \boldsymbol{\alpha}, \boldsymbol{\beta}) \to HF^\circ(\Sigma, \boldsymbol{\alpha}, \boldsymbol{\gamma}) \tag{4.1}$$

Similarly, if $\boldsymbol{\alpha} \sim \boldsymbol{\beta}$, then let $\Psi^{\boldsymbol{\alpha} \to \boldsymbol{\beta}}_{\boldsymbol{\gamma}}$ denote the map

$$F^\circ_{\boldsymbol{\beta},\boldsymbol{\alpha},\boldsymbol{\gamma}}(\Theta_{\boldsymbol{\beta},\boldsymbol{\alpha}} \otimes -) : HF^\circ(\Sigma, \boldsymbol{\alpha}, \boldsymbol{\gamma}) \to HF^\circ(\Sigma, \boldsymbol{\beta}, \boldsymbol{\gamma}) \tag{4.2}$$

We take a moment to compare $Spin^c$-structures on X to those on $X^\#$. Observe that there is a natural restriction map

$$r : Spin^c(X) \to Spin^c(X^\#) \tag{4.3}$$

The restriction map r is surjective, and conversely, a $Spin^c$-structure $\mathfrak{s}^\#$ on $X^\#$ admits a unique extension to X if it is isomorphic to the unique torsion $Spin^c$-structure $\mathfrak{s}_0$ in a neighborhood of $\#^{k_3} S^1 \times S^2$.

Proposition 4.8. *Fix a* $Spin^c$*-structure* $\mathfrak{s} \in Spin^c(X^\#)$*. Let* $\mathcal{H} = (\underline{\Sigma}, \underline{\boldsymbol{\alpha}}, \underline{\boldsymbol{\beta}}, \underline{\boldsymbol{\gamma}}, w)$ *be the pointed* $\mathfrak{s}$*-admissable Heegaard triple constructed as above, and let* $\mathcal{H}' = (\underline{\Sigma}, \underline{\boldsymbol{\alpha}}', \underline{\boldsymbol{\beta}}', \underline{\boldsymbol{\gamma}}', w)$ *be a Heegaard triple which is strongly equivalent to* $\mathcal{H}$ *and which is subordinate to a bouquet for a framed link* $\mathbb{L}$ *as above. Then in the diagram below*

$$\begin{array}{ccc} HF^\circ(\underline{\Sigma}, \underline{\boldsymbol{\alpha}}, \underline{\boldsymbol{\beta}}, \mathfrak{s}_0) & \xrightarrow{F^\circ_{\underline{\boldsymbol{\alpha}},\underline{\boldsymbol{\beta}},\underline{\boldsymbol{\gamma}},\mathfrak{s}}} & HF^\circ(\underline{\Sigma}, \underline{\boldsymbol{\alpha}}, \underline{\boldsymbol{\gamma}}, \mathfrak{s}_{\underline{\boldsymbol{\alpha}},\underline{\boldsymbol{\gamma}}}) \\ \big\downarrow \Psi^{\underline{\boldsymbol{\alpha}}\to\underline{\boldsymbol{\alpha}}'}_{\underline{\boldsymbol{\beta}}\to\underline{\boldsymbol{\beta}}'} & & \big\downarrow \Psi^{\underline{\boldsymbol{\alpha}}\to\underline{\boldsymbol{\alpha}}'}_{\underline{\boldsymbol{\gamma}}\to\underline{\boldsymbol{\gamma}}'} \\ HF^\circ(\underline{\Sigma}, \underline{\boldsymbol{\alpha}}', \underline{\boldsymbol{\beta}}', \mathfrak{s}_0) & \xrightarrow{F^\circ_{\mathbb{L},\mathfrak{s}}} & HF^\circ(\underline{\Sigma}, \underline{\boldsymbol{\alpha}}', \underline{\boldsymbol{\gamma}}', \mathfrak{s}_{\underline{\boldsymbol{\alpha}}',\underline{\boldsymbol{\gamma}}'}) \end{array}$$

we have the following equality

$$F^\circ_{\mathbb{L},\mathfrak{s}} \circ \Psi^{\underline{\boldsymbol{\alpha}}\to\underline{\boldsymbol{\alpha}}'}_{\underline{\boldsymbol{\beta}}\to\underline{\boldsymbol{\beta}}'}(\Theta_{\underline{\boldsymbol{\alpha}},\underline{\boldsymbol{\beta}}}) = \Psi^{\underline{\boldsymbol{\alpha}}\to\underline{\boldsymbol{\alpha}}'}_{\underline{\boldsymbol{\gamma}}\to\underline{\boldsymbol{\gamma}}'} \circ F_{\underline{\boldsymbol{\alpha}},\underline{\boldsymbol{\beta}},\underline{\boldsymbol{\gamma}},\mathfrak{s}}(\Theta_{\underline{\boldsymbol{\alpha}},\underline{\boldsymbol{\beta}}}) \tag{4.4}$$

Proof. Similar results are common in the literature, so we'll be brief (cf. [OS06, p.360]). By assumption, the cut systems $\underline{\boldsymbol{\alpha}} \sim \underline{\boldsymbol{\alpha}}'$, $\underline{\boldsymbol{\beta}} \sim \underline{\boldsymbol{\beta}}'$, and $\underline{\boldsymbol{\gamma}} \sim \underline{\boldsymbol{\gamma}}'$ are related by sequences of isotopies and handleslides. Start by considering the sequence $\underline{\boldsymbol{\alpha}} \sim \underline{\boldsymbol{\alpha}}'$, which yields the following diagram:

$$\begin{array}{ccc} HF^\circ(\underline{\Sigma}, \underline{\boldsymbol{\alpha}}, \underline{\boldsymbol{\beta}}, \mathfrak{s}_0) & \xrightarrow{F^\circ_{\underline{\boldsymbol{\alpha}},\underline{\boldsymbol{\beta}},\underline{\boldsymbol{\gamma}},\mathfrak{s}}} & HF^\circ(\underline{\Sigma}, \underline{\boldsymbol{\alpha}}, \underline{\boldsymbol{\gamma}}, \mathfrak{s}_{\underline{\boldsymbol{\alpha}},\underline{\boldsymbol{\gamma}}}) \\ \big\downarrow \Psi^{\underline{\boldsymbol{\alpha}}\to\underline{\boldsymbol{\alpha}}'}_{\underline{\boldsymbol{\beta}}} & & \big\downarrow \Psi^{\underline{\boldsymbol{\alpha}}\to\underline{\boldsymbol{\alpha}}'}_{\underline{\boldsymbol{\gamma}}} \\ HF^\circ(\underline{\Sigma}, \underline{\boldsymbol{\alpha}}', \underline{\boldsymbol{\beta}}, \mathfrak{s}_0) & \xrightarrow[F^\circ_{\underline{\boldsymbol{\alpha}}',\underline{\boldsymbol{\beta}},\underline{\boldsymbol{\gamma}},\mathfrak{s}}]{} & HF^\circ(\underline{\Sigma}, \underline{\boldsymbol{\alpha}}', \underline{\boldsymbol{\gamma}}, \mathfrak{s}_{\boldsymbol{\alpha}',\boldsymbol{\gamma}}) \end{array}$$

Figure 4.8: The commutative square associated to the sequence of isotopies and handle slides connecting $\underline{\boldsymbol{\alpha}}$ to $\underline{\boldsymbol{\alpha}}'$.

By [JTZ12, Proposition 9.10] we have that both $\Psi^{\underline{\boldsymbol{\alpha}}\to\underline{\boldsymbol{\alpha}}'}_{\underline{\boldsymbol{\beta}}}$ and $\Psi^{\underline{\boldsymbol{\alpha}}\to\underline{\boldsymbol{\alpha}}'}_{\underline{\boldsymbol{\gamma}}}$ are isomorphisms, and by [JTZ12, Lemma 9.4] we have that $HF^\circ_{\text{top}}(\underline{\Sigma}, \underline{\boldsymbol{\alpha}}, \underline{\boldsymbol{\beta}}, \mathfrak{s}_0) \cong \mathbb{F}_2\langle\Theta_{\underline{\boldsymbol{\alpha}},\underline{\boldsymbol{\beta}}}\rangle$ and $HF^\circ_{\text{top}}(\underline{\Sigma}, \underline{\boldsymbol{\alpha}}', \underline{\boldsymbol{\beta}}, \mathfrak{s}_0) \cong \mathbb{F}_2\langle\Theta_{\underline{\boldsymbol{\alpha}}',\underline{\boldsymbol{\beta}}}\rangle$. It is now immediate that $\Psi^{\underline{\boldsymbol{\alpha}}\to\underline{\boldsymbol{\alpha}}'}_{\underline{\boldsymbol{\beta}}}(\Theta_{\underline{\boldsymbol{\alpha}},\underline{\boldsymbol{\beta}}}) = \Theta_{\underline{\boldsymbol{\alpha}}',\underline{\boldsymbol{\beta}}}$.

Using [JTZ12, Lemma 9.5], we may assume that $(\Sigma, \underline{\boldsymbol{\alpha}}', \underline{\boldsymbol{\alpha}}, \underline{\boldsymbol{\beta}}, \underline{\boldsymbol{\gamma}}, w)$ has also been made admissable, so we can apply the associativity theorem for holomorphic triangles [OS04b, Theorem 8.16] and conclude that

$$F^\circ_{\underline{\alpha}',\underline{\alpha},\underline{\gamma}}\big(\Theta_{\underline{\alpha}',\underline{\alpha}}\otimes F^\circ_{\underline{\alpha},\underline{\beta},\underline{\gamma},\mathfrak{s}}(\Theta_{\underline{\alpha},\underline{\beta}}\otimes\Theta_{\underline{\beta},\underline{\gamma}})\big)=F^\circ_{\underline{\alpha}',\underline{\beta},\underline{\gamma},\mathfrak{s}}\big(F^\circ_{\underline{\alpha}',\underline{\alpha},\underline{\beta}}(\Theta_{\underline{\alpha}',\underline{\alpha}}\otimes\Theta_{\underline{\alpha},\underline{\beta}})\otimes\Theta_{\underline{\beta},\underline{\gamma}}\big) \tag{4.5}$$

Clearly, equation (4.5) shows that the diagram in Figure 4.8 commutes for the generator $\Theta_{\underline{\alpha},\underline{\beta}}$.

Having handled the sequence $\underline{\alpha}\sim\underline{\alpha}'$, we consider next the sequence of isotopies and handleslides amongst the $\underline{\beta}$-curves. In a similar fashion, we consider the following diagram

$$\begin{array}{ccc}
HF^\circ(\underline{\Sigma},\underline{\alpha}',\underline{\beta},\mathfrak{s}_0) & \xrightarrow{F^\circ_{\underline{\alpha}',\underline{\beta},\underline{\gamma},\mathfrak{s}}} & HF^\circ(\underline{\Sigma},\underline{\alpha}',\underline{\gamma},\mathfrak{s}_{\underline{\alpha}',\underline{\gamma}}) \\
\downarrow{\scriptstyle \Psi^{\underline{\alpha}'}_{\underline{\beta}\to\underline{\beta}'}} & & \| \\
HF^\circ(\underline{\Sigma},\underline{\alpha}',\underline{\beta}',\mathfrak{s}_0) & \xrightarrow[F^\circ_{\underline{\alpha}',\underline{\beta}',\underline{\gamma},\mathfrak{s}}]{} & HF^\circ(\underline{\Sigma},\underline{\alpha}',\underline{\gamma},\mathfrak{s}_{\alpha',\gamma})
\end{array}$$

Figure 4.9: The commutative square associated to the sequence of isotopies and handle slides connecting $\underline{\beta}$ to $\underline{\beta}'$.

The proof that Figure 4.9 is commutative, however, is slightly different than that for Figure 4.8, so we include the proof here. As before, we apply [JTZ12, Lemma 9.5] to justify that $(\Sigma,\underline{\alpha}',\underline{\beta},\underline{\beta}',\underline{\gamma},w)$ is admissable. Applying the associativity theorem for holomorphic triangles, we see that

$$F^\circ_{\underline{\alpha}',\underline{\beta}',\underline{\gamma}}\big(F^\circ_{\underline{\alpha}',\underline{\beta},\underline{\beta}'}(\Theta_{\underline{\alpha}',\underline{\beta}}\otimes\Theta_{\underline{\beta},\underline{\beta}'})\otimes\Theta_{\underline{\beta}',\underline{\gamma}}\big)=F^\circ_{\underline{\alpha}',\underline{\beta},\underline{\gamma}}\big(\Theta_{\underline{\alpha}',\underline{\beta}}\otimes F^\circ_{\underline{\beta},\underline{\beta}',\underline{\gamma}}(\Theta_{\underline{\beta}',\underline{\beta}}\otimes\Theta_{\underline{\beta}',\underline{\gamma}})\big) \tag{4.6}$$

By again applying [JTZ12, Proposition 9.10] and [JTZ12, Lemma 9.4], we observe that

$$F^\circ_{\underline{\beta},\underline{\beta}',\underline{\gamma}}(\Theta_{\underline{\beta},\underline{\beta}'}\otimes\Theta_{\underline{\beta}',\underline{\gamma}})=\Theta_{\underline{\beta},\underline{\gamma}} \tag{4.7}$$

which turns equation (4.7) into

$$F^\circ_{\underline{\alpha}',\underline{\beta}',\underline{\gamma}}\big(F^\circ_{\underline{\alpha}',\underline{\beta},\underline{\beta}'}(\Theta_{\underline{\alpha}',\underline{\beta}}\otimes\Theta_{\underline{\beta},\underline{\beta}'})\otimes\Theta_{\underline{\beta}',\underline{\gamma}}\big)=F^\circ_{\underline{\alpha}',\underline{\beta},\underline{\gamma}}(\Theta_{\underline{\alpha}',\underline{\beta}}\otimes\Theta_{\underline{\beta},\underline{\gamma}}) \tag{4.8}$$

It is immediate from equation (4.8) that Figure 4.9 commutes for the generator $\Theta_{\underline{\boldsymbol{\alpha}}',\underline{\boldsymbol{\beta}}}$.

Having studied the sequences $\underline{\boldsymbol{\alpha}} \sim \underline{\boldsymbol{\alpha}}'$ and $\underline{\boldsymbol{\beta}} \sim \underline{\boldsymbol{\beta}}'$, we leave it to the reader to build an analogous commutative diagram for the sequence $\underline{\boldsymbol{\gamma}} \sim \underline{\boldsymbol{\gamma}}'$ and top generator $\Theta_{\underline{\boldsymbol{\alpha}}',\underline{\boldsymbol{\gamma}}}$. The proof that it is commutative follows as for the sequence $\underline{\boldsymbol{\beta}} \sim \underline{\boldsymbol{\beta}}'$.

To demonstrate the assertion made in the proposition, we observe that after stacking Figures 4.8 and 4.9 on top of the appropriate diagram for the $\underline{\boldsymbol{\gamma}} \sim \underline{\boldsymbol{\gamma}}'$ sequence, we arrive at a new commutative diagram which is equivalent to equation (4.4). This is so for two reasons: first, by Definition the maps $F^{\circ}_{\underline{\boldsymbol{\alpha}}',\underline{\boldsymbol{\beta}}',\underline{\boldsymbol{\gamma}}',\mathfrak{s}}$ and $F^{\circ}_{\mathbb{L},\mathfrak{s}}$ are equivalent, and second, by [JTZ12, Proposition 9.10] we have

$$\Psi^{\underline{\boldsymbol{\alpha}}\to\underline{\boldsymbol{\alpha}}'}_{\underline{\boldsymbol{\beta}}\to\underline{\boldsymbol{\beta}}'} = \Psi^{\underline{\boldsymbol{\alpha}}'}_{\underline{\boldsymbol{\beta}}\to\underline{\boldsymbol{\beta}}'} \circ \Psi^{\underline{\boldsymbol{\alpha}}\to\underline{\boldsymbol{\alpha}}'}_{\underline{\boldsymbol{\beta}}} \qquad \text{and} \qquad \Psi^{\underline{\boldsymbol{\alpha}}\to\underline{\boldsymbol{\alpha}}'}_{\underline{\boldsymbol{\gamma}}\to\underline{\boldsymbol{\gamma}}'} = \Psi^{\underline{\boldsymbol{\alpha}}'}_{\underline{\boldsymbol{\gamma}}\to\underline{\boldsymbol{\gamma}}'} \circ \Psi^{\underline{\boldsymbol{\alpha}}\to\underline{\boldsymbol{\alpha}}'}_{\underline{\boldsymbol{\gamma}}}.$$

□

Theorem 4.9. *In the diagram below,*

$$\begin{array}{ccc} HF^{\circ}(S^3) & \xrightarrow{\quad F^{\circ}_{X,\mathfrak{s}} \quad} & HF^{\circ}(Y,\mathfrak{s}) \\ \downarrow{\scriptstyle F_1} & & \uparrow{\scriptstyle F_3} \\ HF^{\circ}(\underline{\Sigma},\underline{\boldsymbol{\alpha}},\underline{\boldsymbol{\beta}},\mathfrak{s}_0) & \xrightarrow[F^{\circ}_{\underline{\boldsymbol{\alpha}},\underline{\boldsymbol{\beta}},\underline{\boldsymbol{\gamma}},\mathfrak{s}_{\underline{\boldsymbol{\alpha}},\underline{\boldsymbol{\beta}},\underline{\boldsymbol{\gamma}}}}]{} & HF^{\circ}(\underline{\Sigma},\underline{\boldsymbol{\alpha}},\underline{\boldsymbol{\gamma}},\mathfrak{s}_{\underline{\boldsymbol{\alpha}},\underline{\boldsymbol{\gamma}}}) \end{array}$$

the following equality holds

$$F_3 \circ F^{\circ}_{\underline{\boldsymbol{\alpha}},\underline{\boldsymbol{\beta}},\underline{\boldsymbol{\gamma}},\mathfrak{s}_{\underline{\boldsymbol{\alpha}},\underline{\boldsymbol{\beta}},\underline{\boldsymbol{\gamma}}}} \circ F_1(\Theta) = F^{\circ}_{X,\mathfrak{s}}(\Theta) \tag{4.9}$$

Proof. This follows immediately after combining the construction of $X^{\#}$ with Proposition 4.8, the definitions of the 1- and 3-handle cobordism maps, and the classic results of [OS06] which show that $F_{X,\mathfrak{s}}$ is independent of the handle decomposition of X. □

4.4 The image of the contact class

Fix X to be a smooth, oriented, compact four-manifold with connected boundary $\partial X = Y$. As discussed in Section 2.2, a $(g,k;p,b)$-trisection map $\pi : X \to \mathbb{D}^2$ induces an open book decomposition on its boundary 3-manifold Y. Given the data of such an open book, Honda-Kazez-Matic [HKM09] define a class $c(\xi) \in HF^+(-Y, \mathfrak{s}_\xi)$ and show that $c^+(\xi)$ agrees with the Ozsváth-Szabó contact invariant [OS05] associated to (Y, ξ), where ξ is a contact structure supported by the given open book. In this section, we initiate a study of the relationship between $c^+(\xi)$ and relative trisection maps π inducing an open book which supports ξ.

To begin, fix a $(g,k;p.b)$-trisection map $\pi : X \to \mathbb{D}^2$, and let $(\Sigma, \boldsymbol{\alpha}, \boldsymbol{\beta}, \boldsymbol{\gamma})$ be its associated diagram. Next, construct the associated diagram[1] $(\underline{\Sigma}, \underline{\boldsymbol{\beta}}, \underline{\boldsymbol{\gamma}}, \underline{\boldsymbol{\alpha}}, w)$ as in Subsection 4.2 above. For each $i = g-p+1, \ldots, g(\underline{\Sigma}) = g+p+b-1$, let θ_i, x_i, and y_i be the unique intersection point shown in Figure 4.10 below,

$$\begin{aligned} \theta_i &= \boldsymbol{\beta}_i \cap \boldsymbol{\gamma}_i \cap \overline{\Sigma}_{\boldsymbol{\alpha}} \\ x_i &= \boldsymbol{\gamma}_i \cap \boldsymbol{\alpha}_i \cap \overline{\Sigma}_{\boldsymbol{\alpha}} \\ y_i &= \boldsymbol{\beta}_i \cap \boldsymbol{\alpha}_i \cap \overline{\Sigma}_{\boldsymbol{\alpha}} \end{aligned} \tag{4.1}$$

and let Θ, $\mathbf{x}$, and $\mathbf{y}$ be the corresponding intersection points

$$\begin{aligned} \boldsymbol{\Theta} &= \{\Theta^{(1)}_{\boldsymbol{\beta},\boldsymbol{\gamma}}, \ldots, \Theta^{(g-p)}_{\boldsymbol{\beta},\boldsymbol{\gamma}}, \theta_{g-p+1}, \ldots, \theta_{g+p+b-1}\} \in \mathbb{T}_{\underline{\boldsymbol{\beta}}} \cap \mathbb{T}_{\underline{\boldsymbol{\gamma}}} \\ \mathbf{x} &= \{\Theta^{(1)}_{\boldsymbol{\gamma},\boldsymbol{\alpha}}, \ldots, \Theta^{(g-p)}_{\boldsymbol{\gamma},\boldsymbol{\alpha}}, x_{g-p+1}, \ldots, x_{g+p+b-1}\} \in \mathbb{T}_{\underline{\boldsymbol{\gamma}}} \cap \mathbb{T}_{\underline{\boldsymbol{\alpha}}} \\ \mathbf{y} &= \{\Theta^{(1)}_{\boldsymbol{\beta},\boldsymbol{\alpha}}, \ldots, \Theta^{(g-p)}_{\boldsymbol{\beta},\boldsymbol{\alpha}}, y_{g-p+1}, \ldots, y_{g+p+b-1}\} \in \mathbb{T}_{\underline{\boldsymbol{\beta}}} \cap \mathbb{T}_{\underline{\boldsymbol{\alpha}}} \end{aligned} \tag{4.2}$$

[1] We have intentionally flipped the roles of $\underline{\boldsymbol{\alpha}}$, $\underline{\boldsymbol{\beta}}$, and $\underline{\boldsymbol{\gamma}}$ in this construction, as will be apparent momentarily.

To describe the symbols $\Theta^{(i)}_{\boldsymbol{\xi},\boldsymbol{\zeta}}$, for $i = 1, \ldots, g-p$ and $\boldsymbol{\xi}, \boldsymbol{\zeta} \in \{\boldsymbol{\alpha}, \boldsymbol{\beta}, \boldsymbol{\gamma}\}$, recall that by the connect sum formula [OS04a] and Corollary 4.5, it follows that

$$HF^+(\underline{\Sigma}, \underline{\boldsymbol{\beta}}, \underline{\boldsymbol{\alpha}}, \mathfrak{s}_0) \cong HF^+(\underline{\Sigma}, \underline{\boldsymbol{\gamma}}, \underline{\boldsymbol{\beta}}, \mathfrak{s}_0) \cong \Lambda^*(H_1(\#^{k+2p+b-1} S^1 \times S^2)) \otimes \mathbb{F}_2[U, U^{-1}]/U \cdot \mathbb{F}_2[U] \tag{4.3}$$

and

$$HF^+(\underline{\Sigma}, \underline{\boldsymbol{\gamma}}, \underline{\boldsymbol{\alpha}}, \mathfrak{s}\#\mathfrak{s}_0) \cong HF^+(Y, \mathfrak{s}) \otimes HF^+(\#^k S^1 \times S^2; \mathfrak{s}_0) \tag{4.4}$$

With these observations in mind, we choose the $\Theta^{(i)}_{\boldsymbol{\xi},\boldsymbol{\zeta}}$ so that they represent the top-degree homology class in these decompositions.

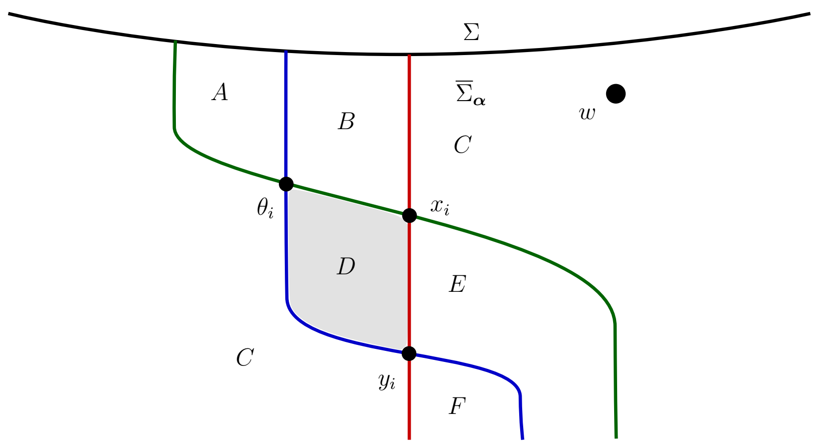

Figure 4.10: A local picture of the intersection points θ_i, x_i, and y_i.

Proposition 4.10. *The generator* $[\mathbf{x}, 0]$ *is a cycle in* $CF^+(\underline{\Sigma}, \underline{\boldsymbol{\gamma}}, \underline{\boldsymbol{\alpha}}, w)$*, and its image in homology is mapped to* $c^+(Y, \xi) \in HF^+(-Y, \mathfrak{s}_\xi)$ *under the* 3*-handle cobordism map. That is,*

$$\begin{aligned} HF^+(-Y^\#, \mathfrak{s}_\xi\#\mathfrak{s}_0) &\xrightarrow{F_3} HF^+(-Y, \mathfrak{s}_\xi) \\ [\mathbf{x}, 0] &\longrightarrow c^+(\xi) \end{aligned}$$

Proof. Let $\boldsymbol{\alpha} = \{\alpha_1, \ldots, \alpha_{g-p}\} \subset \underline{\boldsymbol{\alpha}}$ and $\boldsymbol{\gamma} = \{\gamma_1, \ldots, \gamma_{g-p}\} \subset \underline{\boldsymbol{\gamma}}$ denote the original cut systems arising from $\pi : X \to \mathbb{D}^2$. By assumption, there exists sequences of isotopies and handleslides after which $(\Sigma, \boldsymbol{\gamma}, \boldsymbol{\alpha})$ is a standard diagram. Observe that these sequences can be chosen so as to not interact with the new $\boldsymbol{\alpha}$ and $\boldsymbol{\gamma}$ curves.

Thus, $(\underline{\Sigma}, \underline{\boldsymbol{\gamma}}, \underline{\boldsymbol{\alpha}}, w)$ is slide-equivalent to a stabilized diagram for $Y\#(S^1 \times S^2)^{\#k_3}$ obtained via the Honda-Kazez-Matic procedure after adding two-dimensional 1-handles to the page $\Sigma_{\boldsymbol{\alpha}}$ and extending the monodromy across them by the identity. In particular, [HKM09, Theorem 3] implies that $[\mathbf{x}, 0]$ is a cycle whose image in homology represents the contact class for $(Y^{\#}, \xi_{\#})$. Finally, that $[\mathbf{x}, 0]$ is sent to $c^+(\xi)$ follows from the definition of the three-handle map. □

Theorem 4.11. *The image of* $c^+(\xi)$ *under* $F^+_{\overline{X},\bar{\mathfrak{s}}}$ *coincides with the image of* $[\mathbf{x}, 0]$ *in homology under the map* $F^+_{\underline{\boldsymbol{\beta}},\underline{\boldsymbol{\gamma}},\underline{\boldsymbol{\alpha}}}(\Theta_{\underline{\boldsymbol{\beta}},\underline{\boldsymbol{\gamma}}} \otimes -)$.

Proof. This statement follows quickly from the work done in Subsections 4.2 and 4.3. Namely, the combination of Proposition 4.8 and Proposition 4.10 implies that the following diagram commutes:

$$\begin{array}{ccc} HF^+(-Y, \mathfrak{s}_\xi) & \xrightarrow{\;F^+_{\overline{X},\bar{\mathfrak{s}}}\;} & HF^+(S^3) \\ {\scriptstyle F_3}\uparrow & \nearrow {\scriptstyle F^+_{\underline{\boldsymbol{\gamma}},\underline{\boldsymbol{\beta}},\underline{\boldsymbol{\alpha}},\mathfrak{s}}(\Theta_{\underline{\boldsymbol{\beta}},\underline{\boldsymbol{\gamma}}}\otimes -)} & \\ HF^+(-Y^{\#}, \mathfrak{s}_\xi \# \mathfrak{s}_0) & & \end{array}$$

□

Next, we show how the diagram constructed in subsection above allows us to exhibit some control over the holomorphic triangles which appear in our count. The following is only a slight adaptation of [Bal13, Proposition 2.3] to our current setting.

Proposition 4.12. *Suppose that* $(\underline{\Sigma}, \underline{\boldsymbol{\beta}}, \underline{\boldsymbol{\gamma}}, \underline{\boldsymbol{\alpha}}, w)$ *has been made weakly admissable, and let* ψ *be a homotopy class of Whitney triangles connecting* $\boldsymbol{\Theta}$*,* $\mathbf{x}$*, and any other point* $\mathbf{w} \in \mathbb{T}_{\underline{\boldsymbol{\beta}}} \cap \mathbb{T}_{\underline{\boldsymbol{\alpha}}}$*. If* ψ *admits a holomorphic representative and satisfies* $n_w(\psi) = 0$*, then* $\mathbf{w}$ *must be of the form*

$$\mathbf{w} = \{w^{(1)}, \ldots, w^{(g-p)}\} \cup \{y_{g-p+1}, \ldots, y_{g+p+b-1}\}, \tag{4.5}$$

and $D(\psi) = \sum_{i=1}^{g-p} \Delta'_i + \Delta_{g-p+1} + \cdots + \Delta_{g+p+b-1}$ *where* Δ'_i *are triangles entirely contained in* Σ*.*

Proof. Suppose that ψ has a holomorphic representative and satisfies $n_w(\psi) = 0$. It follows that every coefficient in the domain $D(\psi)$ is non-negative, and that $D(\psi)$ must have multiplicity 0 in the region containing the basepoint w. Moreover, the oriented boundary of $D(\psi)$ consists of arcs along the $\underline{\boldsymbol{\beta}}$ curves from the points $w_{g-p+1}, \ldots, w_{g+p+b-1}$ to the points $\theta_{g-p+1}, \ldots, \theta_{g+p+b-1}$; arcs along the $\underline{\boldsymbol{\gamma}}$ curves from the points $\theta_{g-p+1}, \ldots, \theta_{g+p+b-1}$ to the points $x_{g-p+1}, \ldots, x_{g+p+b-1}$; and arcs along the $\underline{\boldsymbol{\alpha}}$ curves from the points $x_{g-p+1}, \ldots, x_{g+p+b-1}$ to the points $w_{g-p+1}, \ldots, w_{g+p+b-1}$.

Denote by a, b, c, d, e and f the multiplicities of $D(\psi)$ in the regions A, B, C, D, E and F shown in Figure 4.10 above. Observe that $c = 0$. The boundary constraints on D then imply that

$$a + d - b = 1 \tag{4.6}$$

$$d = b + e + 1 \tag{4.7}$$

After subtracting (4.6) from (4.7), we determine that $a = -e$. However, since all coefficients of $D(\psi)$ must be non-negative, it must be that $a = e = 0$. If $w_i \neq y_i$, the constraints on $\partial D(\psi)$ near y_i force $f + d = 0$, which implies that $f = d = 0$. However, plugging this back into (4.6), together with $a = 0$, implies that $-b = 1$, which is a contradiction. Thus, it must be that $w_i = y_i$. Next, the constraints on $\partial D(\psi)$ (together with the fact that $e = c = 0$) near y_i require that $d + f = 1$. Substituting this into (4.7) implies that $d = 1$ and $f = b = 0$. Thus we conclude that $d = 1$ and $a = b = c = e = f = 0$. □

Bibliography

[Akb02] Selman Akbulut. "Variations on Fintushel-Stern knot surgery on 4-manifolds". In: *Turkish Journal of Mathematics* 26.1 (2002), pp. 81–92.

[AK11] Selman Akbulut and Cagri Karakurt. "Action of the cork twist on Floer homology". In: *arXiv preprint arXiv:1104.2247* (2011).

[AM19] José Román Aranda and Jesse Moeller. "Diagrams of*-Trisections". In: *arXiv preprint arXiv:1911.06467* (2019).

[Bal13] John A. Baldwin. "Capping off open books and the Ozsváth-Szabó contact invariant". In: *Journal of Symplectic Geometry* 11.4 (2013), pp. 525–561.

[BS17] R Inanc Baykur and Osamu Saeki. "Simplifying indefinite fibrations on 4-manifolds". In: *arXiv preprint arXiv:1705.11169* (2017).

[Beh14] Stefan Behrens. "Smooth 4-Manifolds and Surface Diagrams". PhD thesis. Universitäts-und Landesbibliothek Bonn, 2014.

[BH12] Stefan Behrens and Kenta Hayano. "Vanishing cycles and homotopies of wrinkled fibrations". In: *arXiv preprint arXiv:1210.5948* (2012).

[BH16] Stefan Behrens and Kenta Hayano. "Elimination of cusps in dimension 4 and its applications". In: *Proceedings of the London Mathematical Society* 113.5 (2016), pp. 674–724.

[CGP18] Nickolas Castro, David Gay, and Juanita Pinzón-Caicedo. "Diagrams for relative trisections". In: *Pacific Journal of Mathematics* 294.2 (2018), pp. 275–305.

[FS98] Ronald Fintushel and Ronald J Stern. "Knots, links, and 4-manifolds". In: *Inventiones mathematicae* 134.2 (1998), pp. 363–400.

[Gay19] David T. Gay. "From Heegaard splittings to trisections; porting 3-dimensional ideas to dimension 4". In: *arXiv preprint arXiv:1902.01797* (2019).

[GK15] David T Gay and Robion Kirby. "Indefinite Morse 2–functions: Broken fibrations and generalizations". In: *Geometry & Topology* 19.5 (2015), pp. 2465–2534.

[GK12] David Gay and Robion Kirby. "Reconstructing 4–manifolds from Morse 2–functions". In: *Geometry & Topology Monographs* 18 (2012), pp. 103–114.

[GK16] David Gay and Robion Kirby. "Trisecting 4–manifolds". In: *Geometry & Topology* 20.6 (2016), pp. 3097–3132.

[GM18] David Gay and Jeffrey Meier. "Doubly pointed trisection diagrams and surgery on 2-knots". In: *arXiv preprint arXiv:1806.05351* (2018).

[Gir02] Emmanuel Giroux. "Géométrie de contact: de la dimension trois vers les dimensions supérieures". In: *Proceedings of the International Congress of Mathematicians, Vol. II (Beijing, 2002).* Higher Ed. Press, Beijing, 2002, pp. 405–414.

[Hay14] Kenta Hayano. "Modification rule of monodromies in an R2–move". In: *Algebraic & Geometric Topology* 14.4 (2014), pp. 2181–2222.

[HKM09] Ko Honda, William H Kazez, and Gordana Matić. "On the contact class in Heegaard Floer homology". In: *Journal of Differential Geometry* 83.2 (2009), pp. 289–311.

[JM08] Stanislav Jabuka and Thomas E Mark. "Product formulae for Ozsváth–Szabó 4–manifold invariants". In: *Geometry & Topology* 12.3 (2008), pp. 1557–1651.

[Joh06] Klaus Johannson. *Topology and combinatorics of 3-manifolds.* Springer, 2006.

[JTZ12] András Juhász, Dylan P. Thurston, and Ian Zemke. "Naturality and mapping class groups in Heegaard Floer homology". In: *arXiv preprint arXiv:1210.4996* (2012).

[JZ18a] András Juhász and Ian Zemke. "Concordance surgery and the Ozsváth-Szabó 4-manifold invariant". In: *arXiv preprint arXiv:1804.06221* (2018).

[JZ18b] András Juhász and Ian Zemke. "Contact handles, duality, and sutured Floer homology". In: *arXiv preprint arXiv:1803.04401* (2018).

[KM20] Seungwon Kim and Maggie Miller. "Trisections of surface complements and the Price twist". In: *Algebraic & Geometric Topology* 20.1 (2020), pp. 343–373.

[Koe17] Dale Koenig. "Trisections of 3-manifold bundles over S^1". In: *arXiv preprint arXiv:1710.04345* (2017).

[Lam19] Peter Lambert-Cole. "Symplectic surfaces and bridge position". In: *arXiv preprint arXiv:1904.05137* (2019).

[LM18] Peter Lambert-Cole and Jeffrey Meier. "Bridge trisections in rational surfaces". In: *arXiv preprint arXiv:1810.10450* (2018).

[LMS20] Peter Lambert-Cole, Jeffrey Meier, and Laura Starkston. "Symplectic 4-manifolds admit Weinstein trisections". In: *arXiv preprint arXiv:2004.01137* (2020).

[LP72] François Laudenbach and Valentin Poénaru. "A note on 4-dimensional handle-bodies". In: *Bulletin de la Société Mathé matique de France* 100 (1972), pp. 337–344.

[Lip06] Robert Lipshitz. "A cylindrical reformulation of Heegaard Floer homology". In: *Geometry & Topology* 10.2 (2006), pp. 955–1096.

[MSZ16] Jeffrey Meier, Trent Schirmer, and Alexander Zupan. "Classification of trisections and the generalized property R conjecture". In: *Proceedings of the American Mathematical Society* 144.11 (2016), pp. 4983–4997.

[MZ17] Jeffrey Meier and Alexander Zupan. "Bridge trisections of knotted surfaces in S^4". In: *Transactions of the American Mathematical Society* 369.10 (2017), pp. 7343–7386.

[MZ18] Jeffrey Meier and Alexander Zupan. "Bridge trisections of knotted surfaces in 4-manifolds". In: *Proceedings of the National Academy of Sciences* 115.43 (2018), pp. 10880–10886.

[OS04a] Peter Ozsváth and Zoltán Szabó. "Holomorphic disks and three-manifold invariants: properties and applications". In: *Annals of Mathematics* (2004), pp. 1159–1245.

[OS04b] Peter Ozsváth and Zoltán Szabó. "Holomorphic disks and topological invariants for closed three-manifolds". In: *Annals of Mathematics* (2004), pp. 1027–1158.

[OS05] Peter Ozsváth and Zoltán Szabó. "Heegaard Floer homology and contact structures". In: *Duke Mathematical Journal* 129.1 (2005), pp. 39–61.

[OS06] Peter Ozsváth and Zoltán Szabó. "Holomorphic triangles and invariants for smooth four-manifolds". In: *Advances in Mathematics* 202.2 (2006), pp. 326–400.

[Won16] Biji Wong. "G-corks & Heegaard Floer Homology". In: *arXiv preprint arXiv:1609.04857* (2016).

[Zem15] Ian Zemke. "Graph cobordisms and Heegaard Floer homology". In: *arXiv preprint arXiv:1512.01184* (2015).